ABSTRACT

ZINK, JASON MICHAEL. Using Modern Photogrammetric Techniques to Map Historical Shorelines and Analyze Shoreline Change Rates: Case Study on Bodie Island, North Carolina. (Under the direction of Dr. Margery F. Overton.)

The efficacy of coastal development regulations in North Carolina is dependent on accurately calculated shoreline erosion rates. North Carolina's current methodology for regulatory erosion rate calculation does not take advantage of emerging GIS, photogrammetric, and engineering technologies. Traditionally, historical shoreline positions from a database created in the 1970s have been coupled with a modern shoreline position to calculate erosion rates. The photos from which these historical shorelines come were subject to errors of tilt, variable scale, lens distortion, and relief displacement. Most of these errors could be removed using modern photogrammetric methods. In this study, an effort was made to acquire and rectify, using digital image processing, prints of the original historical photography for Bodie Island, North Carolina. The photography was rectified using the latest available desktop photogrammetry technology. Digitized shorelines were then compared to shorelines of similar date created without the benefit of this modern technology. Uncertainty associated with shoreline positions was documented throughout the process. It was found that the newly created shorelines were significantly different than their counterparts created with analog means. Many factors caused this difference, including: choice of basemaps, number of tie points between photos, quality of ground control points, method of photo correction, and shoreline delineation technique. Using both linear regression and the endpoint method, a number of erosion rates were calculated with the available shorelines. Despite the differences in position of shorelines of the same date, some of the calculated erosion

rates were not significantly different. Specifically, the rate found using all available shorelines prior to this study was very similar to the rate found using all shorelines created in this study. As a result of this and other factors, it was concluded that a complete reproduction of North Carolina's historical shoreline database may not be warranted. The new rectification procedure does have obvious value, and should be utilized in those locations where there is no existing historical data, or where existing data is thought to be of poor quality. This would especially be the case near inlets or other historically unpopulated areas.

Using Modern Photogrammetric Techniques to Map Historical Shorelines and Analyze Shoreline Change Rates: Case Study on Bodie Island, North Carolina

by

JASON MICHAEL ZINK

A thesis submitted to the Graduate Faculty of
North Carolina State University
in partial fulfillment of the
requirements for the Degree of
Master of Science

CIVIL ENGINEERING

Raleigh

2002

APPROVED BY:

Chair of Advisory Committee

PERSONAL BIOGRAPHY

Jason Michael Zink was born in St. Louis, Missouri on October 3, 1978. He is the only son of Michael and Sharon Zink of Huntersville, North Carolina and a brother to Alison. Jason was a 1996 graduate of the North Carolina School of Science and Mathematics (NCSSM) in Durham, North Carolina. He went on to attend the University of North Carolina at Asheville where, in May 2000, he completed a B.A. in Mathematics. Time was taken off both during and after undergraduate work to backpack the 2200 mile Appalachian Trail, from Georgia to Maine. Jason began graduate work at North Carolina State University in the spring of 2001 and has since pursued a Master of Science degree in Civil Engineering, with a concentration in water resources and coastal engineering. As part of this degree program, Jason has also completed a graduate minor in Geographic Information Systems (GIS).

ACKNOWLEDGMENTS

The author would like to offer his sincere gratitude to Dr. Margery F. Overton and Dr. John S. Fisher for their guidance and support throughout this research. Special thanks also go to Stephen B. Benton of the Division of Coastal Management, who was able to provide significant historical insight into erosion rate mapping procedures. Additional help in data collection was provided by Dr. Robert Dolan of the University of Virginia, as well as Julia Knisel at the Division of Coastal Management. Thanks to all previous and current students involved in the NCSU Kenan Natural Hazards Mapping Program – including Melinda Koser, Desiree Tullos, Rachel Smith, and Tiffany LaBrecque. Perhaps most importantly, the author wishes to thank friends and family who offered support throughout the research process.

TABLE OF CONTENTS

Page

LIST OF TABLES

LIST OF FIGURES

LIST OF ABBREVIATIONS

AEC:	Area of Environmental Concern
CAMA:	Coastal Area Management Act
CRC:	Coastal Resources Commission
DCM:	Division of Coastal Management
DTM:	Digital Terrain Model
EP:	Endpoint method of erosion rate calculation
ESRI:	Environmental Systems Research Institute
FRF:	Field Research Facility
GIS:	Geographic Information Systems
GCP:	Ground Control Point
HWL:	High Water Line
LR:	Linear Regression method of erosion rate calculation
MHWL:	Mean High Water Line
NCDOT:	North Carolina Department of Transportation
NMAS:	National Map Accuracy Standards
NOAA:	National Oceanic and Atmospheric Administration
NOS:	National Ocean Service
NPS:	National Park Service
OGMS:	Orthogonal Grid Mapping System
RMSE:	Root Mean Square Error
USGS:	United States Geological Survey

1. INTRODUCTION

The coastal areas of North Carolina are currently undergoing a dramatic increase in development. Coastal buildings and other infrastructure are susceptible to both sea level rise and the effects of devastating coastal storms. The state of North Carolina regulates the development of the coastal areas with consideration of economic impacts and the safety of residents. An understanding of shoreline erosion trends is necessary when making regulatory decisions concerning coastal development. This requires knowledge of both modern and historical shoreline positions. With current image processing technology, it is easy to generate accurate modern shoreline positions. The generation of historical shorelines presents a much greater challenge. Historical shorelines already exist for much of North Carolina. These shorelines reflect the best technology available at the time of their creation, but could likely be improved upon by modern methods. This study serves to assess the methods, both past and present, used in the creation of shorelines from historical aerial photography. A new photogrammetric method for the creation of historical shorelines is described and evaluated.

1.1. Use of Erosion Rates in Coastal Management Programs

Construction near the oceanfront shoreline is frequently regulated through the use of building setbacks. Setbacks can be established as either “fixed” or “floating”. A fixed setback is one which is unresponsive to local shoreline erosion trends. Fixed setbacks are established at a constant distance from some baseline, such as a contour, mean high water line, or vegetation line. For example, on oceanfront beaches in Delaware, the building setback is 100 feet, measured from the seawardmost 10 foot contour. Under a fixed setback regulation, a severely eroding beach uses the same setback as an accreting beach. Alternatively, nine states utilize a floating setback, which allows the setback to vary across the state's shoreline depending on local erosion trends (Houlihan, 1989). With a floating setback, an erosion rate multiplier, which range from 20 to 100 years, is used to calculate the setback distance. As an example, Virginia has a multiplier of 20 years, so a beach with a long-term annual erosion rate of 2 ft/yr would see a building setback of 40 feet from the primary dune crest, while a beach eroding at 10 ft/yr would have a 200 foot setback. Like fixed setbacks, all floating setbacks rely on some baseline from which the setback is measured.

The setback regulations for North Carolina are established by the Coastal Resources Commission (CRC), which was created as a result of the state's Coastal Area Management Act (CAMA). The regulations developed by CRC are administered by the Division of Coastal Management (DCM). The CRC has designated "Areas of Environmental Concern" (AECs) throughout the state's 20 coastal counties. The setback requirements are included as part of the Ocean Hazard System AEC. These requirements state:

> For small structures or single family homes, the (setback) line extends landward a distance of 30 times the average annual erosion rate at the site. In areas where erosion is less than 2 feet per year, the setback is 60 feet. For large structures, the erosion setback line extends inland from the first line of stable natural vegetation a distance of 60 times the average annual erosion rate at the site. The minimum setback is 120 feet. In areas where the erosion rate is more than 3.5 feet a year, the setback line shall be set at a distance of 30 times the annual erosion rate plus 105 feet (NC DCM website, 2002).

The nature of these rules require that, before a statewide floating setback can be established, the average annual erosion rate must be calculated for the entirety of North Carolina's shoreline.

1.2. Current Method of Calculating Rates in North Carolina

In 1979, North Carolina completed its first comprehensive report of shoreline change rates. Immediately thereafter, the rates were approved by the CRC for use in establishing setbacks (Benton *et al*., 1997). Since the first report, North Carolina has conducted a statewide update of long-term annual erosion rates approximately every 5 years: 1981, 1986, 1992, and 1998. Each update uses similar procedures to the first, which were developed by Dr. Robert Dolan. Dr. Dolan's method, discussed in depth in Section 4.2, measures the shoreline at shore-perpendicular transects located every 164 feet [50 meters] along the coast. This is done for the current shoreline and a historical shoreline from between 1938 and 1945. Through the 1992 erosion rate update, this historical shoreline was a product of Dr. Dolan's COAST database, which contains shorelines of between 5 and 20 different dates for every location on the North Carolina coast. Instead of the COAST shoreline, the 1998 update is utilizing NOS T-sheet shorelines with dates between 1933 and 1952. The erosion rate is then calculated using a simple endpoint method: the shoreline rate of change at a specific transect is equal to the change in shoreline position divided by the change in time. Once erosion rates are calculated for positions every 164 feet along the shore, the rates are smoothed using a 17-transect (2625 feet) running average. The smoothed rate at each transect is defined as the average of the transect's rate and the eight adjacent rates on either side. This smoothing procedure eliminates small scale dynamic shoreline phenomena, such as beach cusps (Benton *et al*., 1997). The smoothed erosion rates are then rounded and blocked into continuous segments which have approximately the same rate. Blocked segments must be composed of at least 8 transects, and are always assigned whole number rates unless a fractional value dominates the block. It is these blocks of whole number rates are used to establish the building setbacks.

1.3. Research Objective

With construction setbacks directly related to the shoreline erosion rate, it is essential that the legislated erosion rates are calculated to be as accurate as possible. If a shoreline segment with an actual long-term erosion rate of 3 ft/yr is incorrectly legislated as having a rate of 2 ft/yr, a structure built at the minimum setback would be vulnerable in 20 years, rather than the intended time span of 30 years. If the situation is reversed, and legislated rates are erroneously large, a property owner would unnecessarily lose the opportunity to build on a non-vulnerable part of their property. Each erosion rate update takes advantage of new data and new technology, so each report claims to reflect greater accuracy and detail than the last (Benton *et al*., 1997). While this is undoubtedly true, there exists potential for further improvement in the accuracy of the resulting shoreline change rates. The COAST database, which was recently abandoned in favor of using the NOS T-sheet, was established in the 1970s through the rectification of historical aerial photography. While this rectification took advantage of the best available techniques at the time, it did not have the benefit of modern scanning and image processing software. Additionally, it used USGS 1:24,000 quad sheets, with high positional uncertainty, as basemaps. The potential horizontal error of approximately 42 feet associated with the COAST data could likely be reduced if the original photos were rectified using modern methods. As part of this study, aerial photography from several dates used in the COAST database is acquired. Each set of photos is scanned, digitally rectified, and mosaicked using ERDAS Imagine software, with highly accurate 1998 orthophotography as a basemap. The shorelines are digitized and compared to COAST shorelines of the same date. Estimated error associated with the shoreline positions is documented throughout the process.

Additionally, despite studies that indicate erosion rates calculated with linear regression provide more accurate results than those found using the endpoint method, more than two-thirds of agencies that manage coasts still use the endpoint method (Honeycutt *et al*., 2001; Fenster and Dolan, 1994). With the several COAST shorelines that exist for every location in the state, North Carolina has an excellent opportunity to improve shoreline change rate accuracy through the use of linear regression. This study assesses the contribution that modern photogrammetric software and a linear regression rate calculation method could make to the accuracy of long-term erosion rates in North Carolina. This is done by first directly comparing each shoreline generated in this study to the COAST shoreline of the same date. Extra attention is given to the comparison between the two June 1992 shorelines, since the methods used to create the existing 1992 shoreline are known in detail. Next, endpoint and linear regression calculations are used to calculate a variety of long-term erosion rates for the study area. Some of these linear regression calculations include the post-Ash Wednesday storm shoreline (March 1962) and other storm-influenced shorelines. This provides insight as to the effect of including post-storm shorelines in erosion rate calculations.

2. BACKGROUND

2.1. History of Aerial Photography

Photogrammetry, defined as the process of creating maps from images, originated in 1913, when Italians produced the first aerial map. Aerial photography itself actually dates to 1858, when the first known aerial photograph was taken from a balloon over France. For the next century, the primary use of aerial photography was the gathering of military intelligence: first during the Civil War, then both World Wars and, more recently, the Cold War (Falkner, 1995). The 1930s saw the beginning of the first commercial aerial mapping companies. Photos, both commercial and military, were taken to be used in a one-time design effort. Little or no thought was given to future use of the photos beyond that for which they were taken. For this reason, various inconsistencies in historical aerial photography are common: camera and scale information are often missing, photos are taken at irregular intervals, and photo quality is often compromised.

Photogrammetry was still a young science when people began using it to study shorelines. Lucke, Eardley, Shepard, and Smith first used aerial photography to observe coastal features in the 1930s and early 1940s (Dolan, 1978). Beach erosion was first analyzed using aerial photography in the late 1950s. Interest in studying shorelines using aerial photography greatly increased after the widespread and devastating Ash Wednesday storm of March 1962. By the late 1960s, a number of studies were under way to quantify shoreline change using measurements taken from aerial photography (Dolan, 1978). These studies, which are discussed in depth in Section 4.2, include those by Stafford and Langfelder (1971), as well as Dolan (1978).

2.2. Sources of Error in Aerial Photography

Prior to discussing the specifics of aerial photography, it is necessary to clarify a few terms related to scale. Scale is defined as the ratio of distance on a photograph or map to its corresponding distance on the ground. As a convention, this report will refer only to scale as a unitless ratio, rather than an equivalence. A photo with an equivalence of 1 inch = 1000 feet will be referred to as a photo with a scale of 1:12,000. In this case, 1 unit of measurement on the photo is equal to 12,000 like units of distance on the ground. When comparing two photos of the same size, the one that shows more ground area is said to be of a smaller scale. A photo of scale 1:12,000 is said to be of larger scale than a photo of scale 1:24,000. This is because the representative fraction of the former (1/12,000) is a larger number than that of the latter (1/24,000).

When photos are taken from a plane, many types of error are inevitable. There are four types of aberrations that must be corrected for before the photos become maplike: variable scale, tilt, radial distortion, and relief displacement (Slama *et al*., 1980).

Variable scale refers to adjacent photos in a flight line having slightly differing scales, due to minor changes in altitude of the plane. The altitude at which the plane flies is deliberately chosen to result in photos of a specific scale. Given the focal length of the camera and the desired scale of photography, the required altitude of the plane can be determined by dividing the focal length by the desired scale. For example, if a camera has a focal length of 6 inches (0.5 ft) and the intended scale is 1:12,000, the altitude of the camera is defined by (0.5/(1/12,000)), which equals 6000 feet above average ground level. Despite the plane trying to remain at a constant height of 6000 feet, variations in altitude of up to 1% over a flight line are possible for historical photography missions. The advent of modern

GPS technology has resulted in more precisely controlled flights. For an historical photo, it would not be uncommon for one photo to be taken at an altitude of 6000 feet, while the next is taken at 5990 feet. This would result in neighboring photos having scales of 1:12,000 and 1:11,980, respectively. Treating both of these photos as if they were both of scale 1:12,000 would result in error in the 1:11,980 photo. In this example, if a point is matched on the photos, another point three inches away on the 1:11,980 photo would be subject to an ground error of 5 feet. Such inconsistencies must be removed before the photos can be treated as maplike.

Similarly, changes in the tilt of the airplane result in a variable scale within a photo. Despite trying to remain completely level during the flight, the airplane experiences occasional changes in pitch. If either wing dips slightly toward the ground, the result would be tilt in the x-direction of the photo. Likewise, tilt in the y-direction would result from the nose of the plane tipping toward or away from the ground. If the left wing of the plane is tilted slightly toward the ground, the left side of the resulting photo would have a larger scale than the right side. About half of the near-vertical air photos taken for domestic mapping purposes are tilted less than 2 degrees, and few are tilted more than 3 degrees (Slama et al., 1980). Two or three degrees of tilt can result in a quite large displacement of features on a photo. The following relationship exists to calculate displacement of any point of a photo due to tilt (Anders and Leatherman, 1982):

$$D_t = \frac{Y^2 (\sin T)(\cos P)}{F - (Y \sin T)(\cos P)}$$

where Y is the distance from the point of interest to the isocenter, F is the focal length of the camera, T is angle of tilt, and P is angle between principal line and radial line from the isocenter to the point (as shown in Figure 2-1). The isocenter is the center of radiation for displacement of images due to tilt. The principal line represents the intersection of the photograph with the principal plane, where the principal plane is the plane perpendicular to the tilted photograph. The radial line refers to any line drawn radially from the center point on a vertical photo.

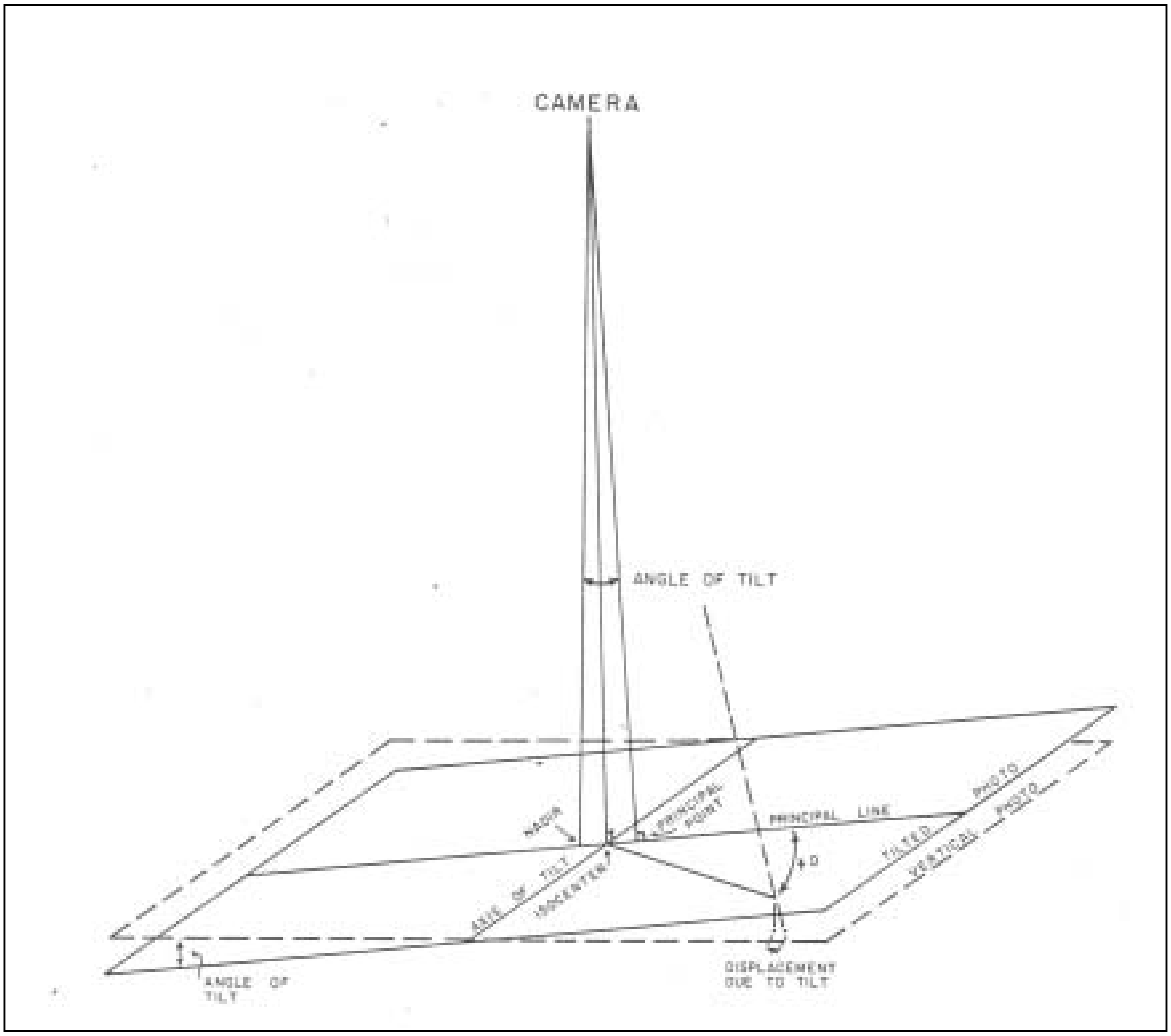

Figure 2-1. Effect of tilt on aerial photography.

Using this relationship, a point on the hypothetical photograph described above (scale 1:12,000, focal length of 0.5 ft), with Y = 3 inches and P = 40 degrees, would be displaced 20 feet from its true ground location as a result of only 1 degree of tilt. If the photo were to be tilted 3 degrees, the horizontal error would be greater than 60 feet. Current aerial photography takes advantage of gyroscopic technology to steady the camera and avoid extreme tilt. However, with historical aerial photography, tilt can account for a significant portion of the error within a photograph.

Radial lens distortion consists of the linear displacement of image points radially from the image center. This is a result of objects at different angular distances from the lens axis undergoing different magnifications (Slama *et al*., 1980). Generally, the older the photography, the greater the error due to radial lens distortion. Correction of radial lens distortion ideally requires knowledge of the specific camera lens used, but non-linear rectification models can closely approximate a solution. Since modern cameras are outfitted with lenses of higher quality, lens distortion has become less of a problem in more recent photography.

Relief displacement occurs as a result of trying to capture a three-dimensional surface as a two-dimensional image. Points on the photo which are elevated above the average ground elevation are displaced outward from the center of the photo. In studies on the east coast of the United States, the terrain is mostly flat, and this is a minimal problem (Gorman *et al*., 1998; Stafford and Langfelder, 1971). However, in choosing ground control points (GCPs) for rectification, care must be taken to avoid using points with an elevation that differs considerably from the mean elevation in the photograph. These would include rooftops of buildings, trees, telephone poles, and features on the crests of dunes.

2.3. Rectification Methods

The process of rectification refers to the matching of coordinates in the image space of the photo to the appropriate coordinates on the object space of the ground. There are three categories of geometric rectification: rubbersheeting, polynomial transformations, and orthorectification. Each category addresses the four sources of error with increasing complexity. The most basic method, rubbersheeting, refers to the linear stretching or shrinking of an image to align it with given control points. This method can correct for scale variations, but is not able to fully account for displacements due to tilt. Lens distortion and radial displacement are not considered in the rubbersheeting process. Since tilt causes differential scale distortion across the photograph, it cannot be compensated for by shrinking or stretching in one direction. A successful polynomial transformation will eliminate error due to scale variation, tilt, and lens distortion. In order to correct for relief displacement, detailed 3-dimensional topographical information must be known. This can be accomplished through the stereoscopic viewing of overlapping pairs of images. More recently, 3-dimensional information can be gathered from a Digital Elevation Model (DEM), which contains elevation data for a dense collection of points. When all four aforementioned sources of error are corrected, including relief displacement, the photo is said to be orthorectified. At this point, the photo is maplike, and distance can be accurately measured.

Before computers were used as an image processing tool, there were a number of mechanical instruments used to adjust photography. One of these was the Zoom Transfer Scope (ZTS). The ZTS uses lenses, mirrors, and lights to change the scale of an image so that it can be superimposed on a basemap (normally a USGS quad sheet). This was done by working in a small area of the photograph to identify a control point that can also be found on the basemap. The image was linearly stretched such that the control point on the image coincided with the same location on the basemap. After this was done for a number of control points, the image was considered to be rectified, and the shoreline was traced. This procedure has been limited in its accuracy by the failure to correct for tilt and relief displacement.

In the 1990s, a number of digital image processing tools were being developed. Among the people developing these were Intergraph, ERDAS, and an enterprise by Thieler and Danforth. By 1993, the entire rectification procedure could be conducted digitally within Intergraph's Imager software (Hiland *et al*., 1993). This allowed for, among other things, viewing images as stereo pairs. Thieler and Danforth, in 1994, presented their Digital Shoreline Mapping System and Digital Shoreline Analysis System (DSMS/DSAS). This method allowed a user to scan photography, select control points and fiducials, and enter camera calibration information. This data was then input into the General Integrated Analytical Triangulation Program (GIANT), created by NOS. The program solved for camera location and orientation at the moment of photography, which was used to derive real-world coordinates for the shoreline. Since the exact position, roll, pitch, and yaw were known for the camera at the moment of photography, tilt could be precisely measured and corrected. This procedure is very similar to that used by ERDAS Imagine 8.5, the software used in this study. ERDAS first introduced a PC-based image processing software in 1978. Since that time, the process has become more automated and accurate. With Imagine 8.5, like DGMS/DGAS, ground control points must be specified by the user. Improvements in image recognition technology allow Imagine to automatically generate a large number of tie points between overlapping images. The use of both tie points and ground control points in this project resulted in a nearly seamless matching of adjacent images. Specific procedures are discussed in Section 5. With the procedure used in this study, images are corrected for all errors except for relief displacement, which is known to be minimal in the study area.

3. STUDY AREA

3.1. Bodie Island, North Carolina

Bodie Island is a barrier island within the Outer Banks, on the northern coast of North Carolina, as seen in Figure 3-1. It is neighbored by Oregon Inlet and Pea Island to the south. The island is not bordered by an inlet to the north, but rather by the towns of Nags Head, Kill Devil Hills, and Kitty Hawk. The next inlet to the north is the entrance to Chesapeake Bay in Virginia, more than 50 miles distant.

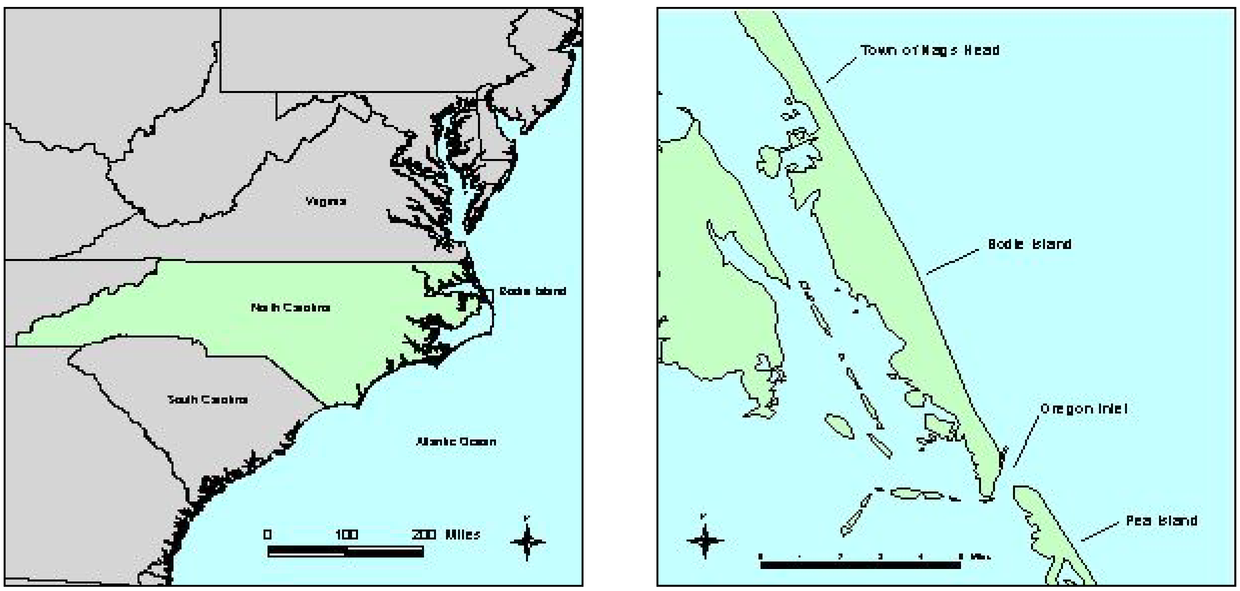

Figure 3-1. Location maps: Bodie Island, North Carolina.

Oregon Inlet opened during a storm in September 1846, though inlets have existed in the vicinity since 1808 (Cleary, 1999). Over the long-term, the effect of Oregon Inlet has been "to induce greater, and more predictable erosion rates adjacent to it than elsewhere" (Everts and Gibson, 1983). In addition to the predictability of erosion rates, there are several factors that make Bodie Island a desirable location for a shoreline change study. The southernmost four miles of shoreline are protected from development by their inclusion in the Cape Hatteras National Seashore. North of the National Seashore, residential development was generally absent until the 1960s. Nonetheless, there are enough enduring structures (roads, houses, lighthouse, Coast Guard Station) to provide sufficient control for photo georeferencing. Figure 3-2 is recent oblique photography which shows Oregon Inlet and the National Seashore portion of Bodie Island.

Figure 3-2. Oblique aerial photo of Bodie Island and Oregon Inlet, April 6, 1999. The terminal groin on the north end of Pea Island can be seen in the lower right.

3.2. Storm History

The North Carolina shoreline has frequently been affected by coastal storms. The tropical cyclones of late summer and fall are perhaps the most well known, but extratropical storms such as nor'easters during winter and early spring have caused just as much beach erosion. Between 1886 and 1996, 166 tropical cyclones (defined as a tropical storm or hurricane) passed within 300 miles of the North Carolina coast. Twenty-eight of these have made landfall in North Carolina (NC State Climate Office website, 2002). Storms such as these have been one of the major factors in short-term shoreline change. Before shoreline positions are to be used in a long-term shoreline study such as this, it is necessary to consider whether the data has been influenced by recent storms. The US Army Corps of Engineers Field Research Facility (FRF), located just north of the study area at Duck, North Carolina, has continually kept wave and wind records since 1980. The FRF defines a storm to be an event in which the significant wave height at gage at the end of their pier exceeds 6.56 feet [2 meters]. Table 3-1 lists storms which occurred within one month of each shoreline date used in this study. Most data in this table was assembled as part of a shoreline study on the Outer Banks of North Carolina (Dolan, 1992), with the more recent dates investigated through the FRF data. Of the six dates with storms in the prior month, all but the 1962 storm were minor, with significant wave heights very close to the minimum criterion of 6.56 feet. Since the decision was made to use the 1992 shoreline to legislate erosion rates in North Carolina's 1992 erosion rate update, it was likely that this shoreline did not show characteristics of a post-storm shoreline. These post-storm dates will initially be included in the database of shorelines used in rate calculations. As part of this study, erosion rates were also calculated without these post-storm shorelines. The sixth storm listed above is of a much larger

Table 3-1. Pertinent storm events.

Date of Shoreline	**Date of Prior Storm (within one month)**	**Storm duration (hours)**	**Average Wind Speed (knots)**	**Significant Wave Height (feet)**
July 1,1945	None			
December 1,1949	Unknown			
October 10,1958	October 3, 1958	29	23	10.2
March 13&14, 1962	March 8, 1962	44	44	29.9
December 5&13, 1962	None			
October 3, 1968	None			
November 6, 1972	Unknown			
June 4, 1974	June 4,1974	15	18	5.9
October 21, 1980	None			
September 19,1984	September 14, 1984	24-48	20	7.9
August 18, 1986	August 17, 1986	22	27	11.2
October 1, 1986	None			
June 17, 1992	May 19, 1992	24	Unknown	8.2
July 22, 1998	None			

magnitude. The storm of March 8, 1962, known as the Ash Wednesday storm, battered the North Carolina coast for days with winds up to 60mph (The Weather Channel website, 2002). As a result of this storm, the Outer Banks were subject to frequent dune failure and overwash. A March 13, 1962 post-storm shoreline exists in the COAST database, and another will be created from March 14, 1962 aerial photography. Erosion rates have been calculated in this study with and without the inclusion of these shorelines. The comparison of the different erosion rates provides some insight as to the effect of including post-storm shorelines in linear regression rate calculations.

4. DATA AND SOFTWARE

Table 4-1 is a summary of shoreline data used in this study. The origins and potential error of each data source are explained in the sections that follow.

Table 4-1. Summary of shoreline data.

Shoreline Date	Source	Maximum Horizontal Error
July 1, 1945	COAST database	42.2 feet
December 1, 1949	NOS T-sheet	34.9 feet
October 10, 1958	COAST database	42.2 feet
March 13, 1962	COAST database	42.2 feet
March 14, 1962	Aerial photography	To be determined
December 5, 1962	Aerial photography	To be determined
December 13, 1962	COAST database	42.2 feet
October 3, 1968	COAST database	42.2 feet
November 6, 1972	Aerial photography	To be determined
June 4, 1974	COAST database	42.2 feet
October 21, 1980	Aerial photography	To be determined
October 21, 1980	COAST database	42.2 feet
September 19, 1984	Aerial photography	To be determined
September 19, 1984	COAST database	42.2 feet
August 18, 1986	COAST database	42.2 feet
October 1, 1986	Aerial photography	To be determined
October 1, 1986	COAST database	42.2 feet
June 17, 1992	Aerial photography	To be determined
June 17, 1992	DCM	42.2 feet
July 22, 1998	DCM	0.5 feet

4.1. GIS and Image Processing Software

The use of a geographic information system (GIS) was integral to the data collection and analysis procedures. A GIS allowed for collecting, storing, retrieving, transforming, and displaying spatial data. ArcView 3.2 and ArcGIS 8 software, both products of Environmental Systems Research Institute (ESRI), were used in this project. This software allowed for rapid display, reprojection, and analysis of existing shorelines and the digitization of new shorelines from rectified images. A number of scripts and extensions were downloaded from ESRI and used to enhance the capabilities of ArcView 3.2. One of these, the ArcView Image Analysis extension, performed rubbersheeting, mosaicking, and other basic image processing functions. It was originally thought that this tool would be used for image rectification in this project. The Image Analysis Extension, jointly created by ESRI and ERDAS, only represented a sampling of the image processing tools available in ERDAS Imagine software. For this reason, ERDAS Imagine 8.5 was used for photo processing. This software used camera information, tie points, ground control points, and topographic data to mathematically establish a relationship between the image space of the photo and the object space of the real world. This has resulted in a highly accurate, seamless matching of a block of photos. Within this project, camera and topographic information were largely unavailable, so the full potential of this software was not explored. Even with this limited use of ERDAS Imagine, it has become clear that it is a valuable tool in desktop photogrammetry.

4.2. COAST Data Sets

After aerial photography began to emerge as a primary tool for studying shorelines, Stafford and Langfelder, in 1971, compiled a list of available aerial photography for the North Carolina coast. Sources of photography included: the Agricultural Stabilization and Conservation Service, the Soil Conservation Service, the U.S. Coast and Geodetic Survey, the U.S. Geological Survey (USGS), the Army Corps of Engineers, and the North Carolina State Highway Commission. After acquiring selected photos, the study established stable reference points every 1000 feet along the beach. The same reference points were identified for each date of photography. Distance was then measured along a shore-perpendicular line from the reference point to the high water line, seen on the photos as the wet/dry line. Since these shore-parallel lines were consistent throughout all photo dates, erosion rates could be computed by dividing the change in distance along the line by the change in time between photos. Thus, erosion rates were computed at locations every 1000 feet along the North Carolina coast. This method, established by Stafford, was a landmark procedure in coastal studies, but was limited by its poor spatial resolution and variable accuracy (Benton *et al.*, 1997). The Stafford method was improved upon in 1978, when the Coastal Research Team at the University of Virginia created the Orthogonal Grid Mapping System (OGMS). With the OGMS method, the historical photography and the corresponding 1:24,000 USGS quad sheet were both enlarged to a scale of 1:5000. A grid with square cells of width 328 feet [100 meters] was drawn on a sheet of tracing paper. The wet/dry line was then traced from the enlargement of the photography. Both the grid and the shoreline tracings were then overlaid on the USGS map enlargement. The long axis of the quad sheet was designated as a baseline, and the distance from the shoreline to the baseline was measured at a point every 328 feet (Dolan, 1978). The OGMS method was adopted by the DCM in 1979 as the procedure to determine official shoreline erosion rates for the state of North Carolina. Specifically, shore-parallel baselines were drawn offshore for the entire coast of North Carolina. One hundred fifty-two baselines, each of approximate length 12,000 feet [3650 meters], were required to span the state's coastline. Beginning in 1981, there existed 72 perpendicular transects for each baseline, spaced at 164 feet apart (rather than the original 328 feet). Dr. Dolan created a personal computer version of this database for DCM use, known as the COAST database. For every date of photography in the database, the distance between the shoreline and the baseline was recorded at each transect. The dates of shorelines in the database depend on the available aerial photography, and therefore vary throughout the state. The study area for this project covers portions of the basemaps known as HAT35, HAT36, HAT37, and HAT38. Figure 4-1 depicts these four basemaps overlaid on the COAST shoreline from December 13, 1962. A noticeable shift in the shoreline occurs between basemaps HAT36 and HAT37. This is not uncommon in shorelines from the COAST database, and will be discussed further in Section 6.1.

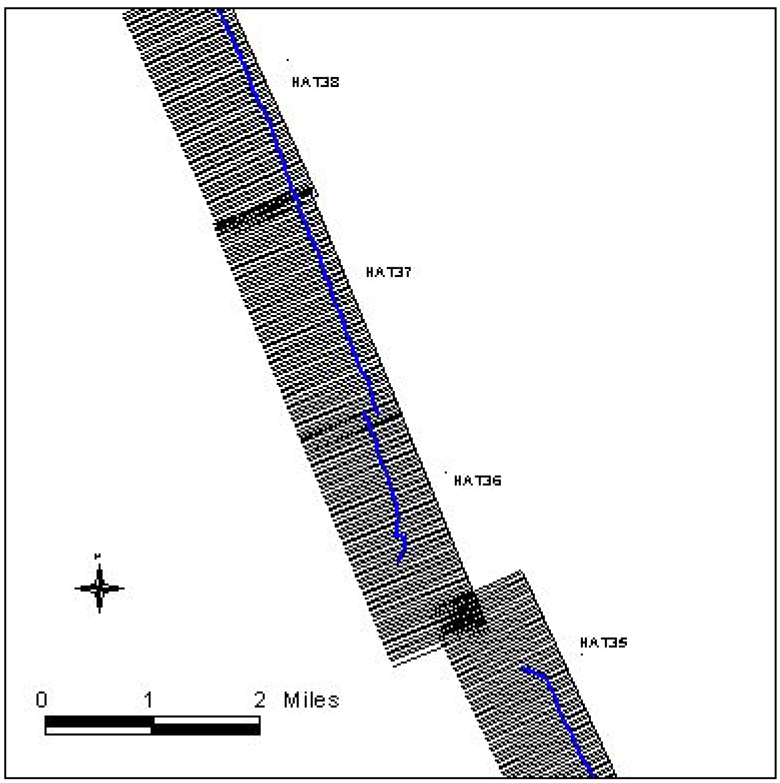

Figure 4-1. Basemaps HAT35, HAT36, HAT37, and HAT38 overlaid on the COAST shoreline of December 13, 1962.

For these basemaps, COAST shorelines are available for the following dates: July 1, 1945; October 10, 1958; March 13, 1962; December 13, 1962; October 3, 1968; June 4, 1974;

October 21, 1980; September 19, 1984, August 18, 1986; October 1, 1986; and June 17, 1992. ArcView shapefiles were created for each of the shorelines in a coordinate system of North Carolina State Plane feet, with NAD83 as the horizontal datum. The maximum potential error for the COAST data has been recognized as 42.16 feet [12.85 meters]. This represents errors from the photographic process, mechanical measurement error, and error in matching photographs to ground features (Dolan, 1980). The DCM, in considering the use of this method to calculate erosion rates in North Carolina, compared the OGMS database to data from many other sources, including a 1978 National Park Service (NPS) study and an Army Corps of Engineers design study for the Oregon Inlet jetties. This comparison resulted in close correlation in all cases, and almost exact correlation of results in some (Dolan *et al*., 1980).

4.3. T-sheet Data Sets

Since the 1830s, the National Ocean Service (previously the National Ocean Survey) has produced coastal maps to aid in marine navigation. These NOS Topographic (T) sheets precisely define the shoreline and many nearshore features, such as rocks, bulkheads, jetties, piers, and ramps (metadata from NOAA). The maps exist at scales of 1:5000, 1:10,000, 1:20,000, and 1:40,000; though 1:10,000 and 1:20,000 T-sheets are the most common (Anders and Byrnes, 1991). Prior to 1927, the shoreline was surveyed using plane table methods. Since 1927, most of the maps have been produced using aerial photography. An approximation of the high water line has always been used as the shoreline in the creation of T-sheets (Shalowitz, 1964). A recent effort, led by the National Oceanic and Atmospheric Administration (NOAA) National Ocean Service, Coastal Services Center, has converted numerous historical T-sheets into digital format. According the shapefile metadata provided from NOAA, the original paper maps were scanned at a resolution of 400dpi. The scanned images were then georeferenced to a number of ground control points, using the image processing capabilities of ESRI's ArcInfo software. The resulting raster image had geographic coordinates in decimal degrees and was referenced to the North American 1983 Datum (NAD83). The shoreline and other features were then digitized as vectorized ArcInfo coverages. Shown in Figure 4-2 are the scanned raster and vectorized versions of T-sheet T9278, which covers the southern end of Bodie Island.

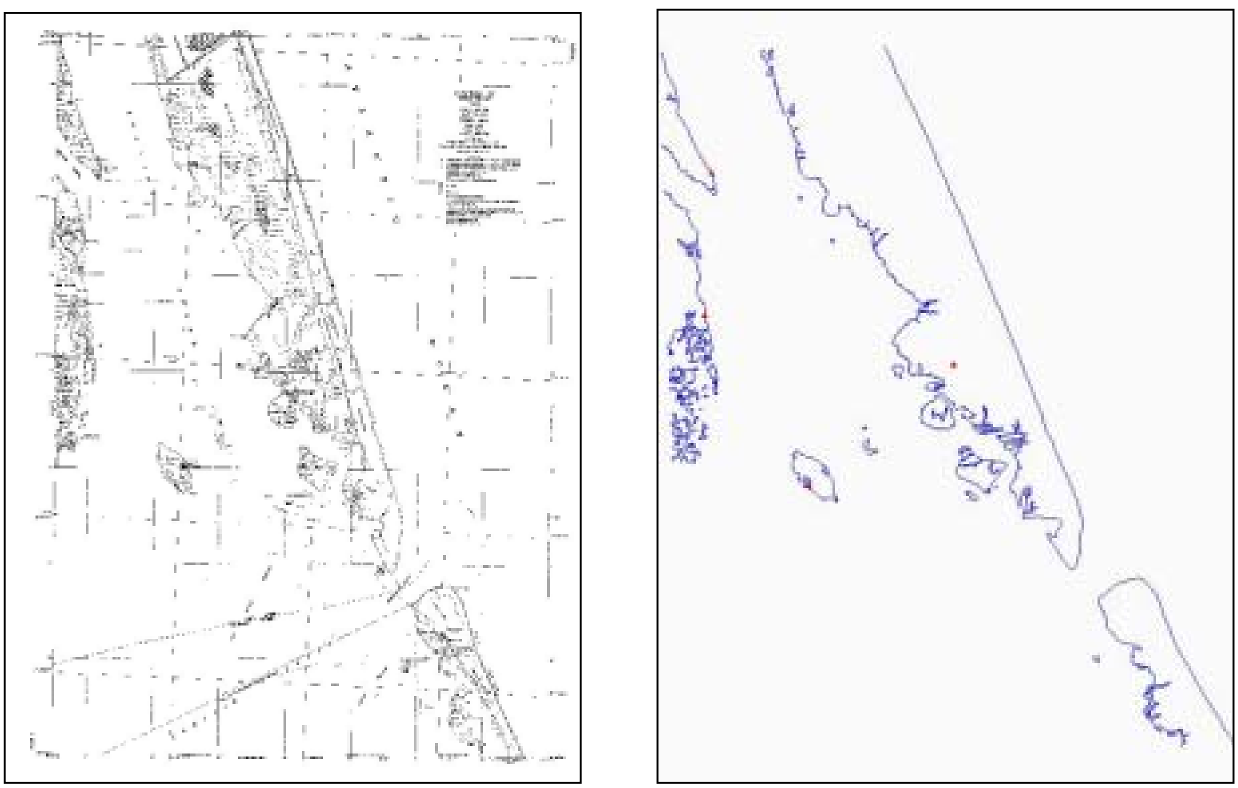

Figure 4-2. Scanned (left) and digitized (right) images of T-sheet T9278. Red triangles are control points from the original T-sheet.

The NOAA project has resulted in digital T-sheet shorelines for virtually all of the North Carolina coast. Dates for these T-sheets range from 1933 to the 1970s, though there are frequently multiple T-sheet shorelines for a given location. The entire state, with the exception of Currituck County, is covered by a T-sheet of a date between 1933 and 1952. It is this shoreline that is being using in North Carolina's current erosion rate update, as described in Section 1.3. In the current T-sheet data set, only a December 1, 1949 shoreline exists for the study area. This T-sheet, T9278, was originally produced at a scale of 1:20,000.

The accuracy of the shoreline on T-sheets is dependent on the era in which the T-sheet was produced. Those created prior to 1941 are subject to a maximum error of +/- 0.4 inches [1 mm] at map scale, which translates to +/- 66 feet [20 meters] at a scale of 1:20,000 (Shalowitz, 1964). All maps created since 1941 meet or exceed the National Map Accuracy Standards (NMAS) of 1941. The NMAS states:

> For maps on publication scales larger than 1:20,000, not more than 10 percent of the points tested shall be in error by more than 1/30 in [0.846 mm] measured on the publication scale; for maps on publication scales of 1:20,000 or smaller, 1/50 in [0.508 mm]. These limits of accuracy shall apply in all cases to positions of well-defined points only. Well-defined points are those that are easily visible or recoverable on the ground, such as the following: monuments or markers, such as benchmarks, property boundary monuments; intersections of roads, railroads, etc.; corners of large buildings or structures (or center points of small buildings); etc.

The NMAS has set even stricter standards for T-sheets, since they are used in navigation. Under these stricter rules, the shoreline at map scale must always be correct within 0.2 inches [0.5 mm] and points used in navigation must be correct within 0.1 inches [0.3 mm] (Ellis, 1978). At a scale of 1:20,000, this translates into a maximum error of +/- 33 feet [10 meters] for the T-sheet shoreline, and +/- 20 feet [6 meters] for points on the T-sheet. Given these maximum allowable errors, a number of studies have evaluated the accuracy of historical T-sheets. Everts, Battley, and Gibson (1983) checked 36 point and shoreline features, and found that the NMAS standards were exceeded by all. For a study site in Delaware, Galgano (1989) found that errors in shoreline position did not exceed 10 feet [3 meters] at a scale of 1:20,000.

The error defined by NMAS was applicable to the original paper maps. Additional error was introduced when NOAA scanned and georeferenced the paper maps. This resulted in a different error for each T-sheet, depending on the quality and quantity of control points available in the georeferencing procedure. The metadata for T9278 reported a horizontal positional accuracy of 0.587 feet [0.179 meters] for x-coordinates, and 2.00 feet [0.609 meters] for y-coordinates. Thus, the composite root mean square error (RMSE) is 2.08 feet [0.635 meters]. The maximum potential error for T9278 is additive, and therefore 34.9 feet [10.64 meters].

4.4. Newly Acquired Photography

An effort was made to acquire unrectified historical aerial photography for the study area. Since the resulting positions and erosion rates were to be compared with rates found with the COAST data, it was desirable to find photos that covered a time span at least as long as that of the COAST data set. Additionally, finding the original photography used in the creation of the COAST data would afford a direct comparison between historical and modern rectification techniques. With these criteria in mind, a search was made for available photography. The final set of photography acquired for use in this study is summarized in Table 4-2:

Table 4-2. Aerial photography acquired for rectification.

Date of Photography	Photo Scale	Photo numbers	Notes
March 14, 1962	1:12,000	128,130-135	One day from COAST date
December 5, 1962	1:6,000	79-85	Eight days from nearest COAST date
November 6, 1972	1:12,000	136-143	No nearby COAST date
October 21, 1980	1:12,000	3874-3876,3879	Same as COAST date
September 19, 1984	1:24,000	271-275	Same as COAST date
October 1, 1986	1:12,000	63-69	Same as COAST date
June 17, 1992	1:12,000	646-655	Same as COAST date

All photos were used as 9 inch by 9 inch black and white prints. With the exception of the 1972 photos, each of the seven sets of photography chosen for rectification was very close in date to a shoreline in the COAST database. Other than the 1972 photos, the largest discrepancy in date was eight days, between the COAST date of December 5, 1962 and the acquired photo date of December 13, 1962.

5. METHODOLOGY

5.1. Image Processing

The image processing portion of the study involved scanning, rectifying, and mosaicking the aerial photographs. Figure 5-1 is a flowchart that summarizes the major operations within the image processing procedure. Each specific operation in the flowchart is explained in detail in the paragraphs that follow.

Each of the 9”x9” aerial photos was first scanned at 1200 dpi using an EPSON Expression 1640XL flatbed scanner. Previous coastal studies used a wide range of scanning resolutions, including 400dpi (Hiland *et al*., 1993), 725dpi (Moore, 2000), and 1693dpi (Overton and Fisher, 1996). Such a variation implied that resolutions have been chosen based on available disk space and time, with little consideration given to photogrammetric standards. It has been suggested that scanned image quality does not increase substantially beyond a magnification level of five (Greve, 1996). When this magnification level of five was applied to the photos in this study, the resulting scanning resolution was 1200dpi. This was within the range of resolutions used by most organizations in the photogrammetric field (Johnston, 2002). Experience suggested that a scanning resolution much higher than 1200dpi would result in exceedingly large file sizes and processing times. When the scanning resolution and the photo scale are known, the resulting pixel size, in inches, was calculated by dividing the scale denominator by the resolution. Table 5-1 lists the pixel sizes for each of the photos used in this study. As a comparison, the 1998 orthophotography, which was used as ground control, was produced with a half-foot pixel size. Immediately following the scanning, each image was cropped and saved as an uncompressed TIFF file. File sizes averaged about 125MB for each scanned 9”x9” photo.

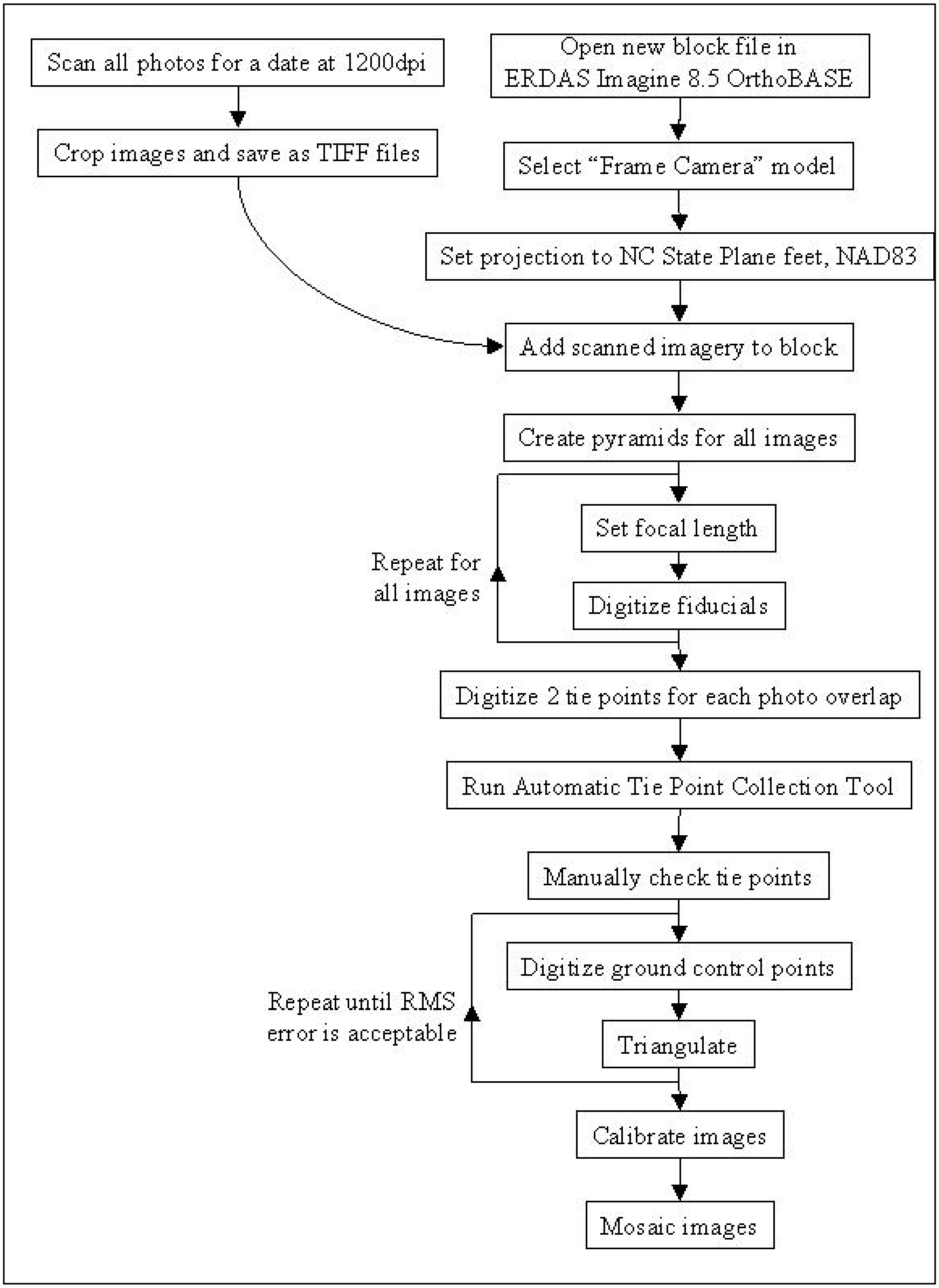

Figure 5-1. Flowchart of image processing procedures.

Table 5-1. Pixel size for scanned photos.

Photo date	Photo scale	Scanning resolution/Pixel size	Ground pixel size
March 14, 1962	1:12,000	1200dpi/21 microns	0.83 feet
December 5, 1962	1:6,000	1200dpi/21 microns	0.42 feet
November 6, 1972	1:12,000	1200dpi/21 microns	0.83 feet
October 21, 1980	1:12,000	1200dpi/21 microns	0.83 feet
September 19, 1984	1:24,000	1200dpi/21 microns	1.67 feet
October 1, 1986	1:12,000	1200dpi/21 microns	0.83 feet
June 17, 1992	1:12,000	1200dpi/21 microns	0.83 feet

The general procedure for creating a rectified mosaic from individual scanned photographs requires successively establishing three types of orientation: interior, exterior, and absolute. Interior orientation is established once the focal length of the camera and the location of the principal point are known (Mikhail *et al*., 2001). Exterior orientation is defined by knowing the positional (x,y,z) and rotational (phi, omega, kappa) coordinates for the camera at the moment of photography (Slama, 1980). Once interior and exterior orientations are known, absolute orientation can be established by relating the coordinates in the image space of the photo to real-world ground coordinates. A fourth type of image orientation, relative orientation, refers to using two images of the same ground area to stereoscopically create a three-dimensional representation.

For each of the seven dates of photography, a block file was created in ERDAS Imagine OrthoBASE. The block file, analogous to the project file in ArcView, stored the file references to all image files and provides an interface in which to conduct all following steps. The block file required that the camera type and camera focal length are specified. Since little camera information was known, a "frame camera" was chosen as the camera model. In this case, the fiducials on the corners of each photo were digitized. The software then identified the principal point of each photo at the intersection of lines connecting opposite fiducials. A focal length of 6 inches [152 mm] was specified for all dates of photography, unless written information on the photos indicated otherwise. As the focal length of the camera for the few photos that did have camera information, 6 inches was a reasonable guess for the remaining photos. The focal length and the digitized fiducials were sufficient for Imagine to determine the interior orientation. Pyramid layers were then created for each image, which allow for faster image viewing at variable scales (ERDAS website, 2002). This automated procedure required each image to successively be resampled at a larger pixel size. For example, pyramid creation at a power of 2 would required that an image at a resolution of 1200dpi was resampled at resolutions of 600dpi, 300dpi, 150dpi, etc.

Prior to establishing ground control for the photos, it was necessary to properly reference the images to each other. This was done through Imagine's Automatic Tie Point Collection tool. Rather than the traditional method of manually identifying several points common to overlapping photographs, the software automatically searched and aligned groups of like pixels on different images. Establishing the interior orientation of each image was a prerequisite to running this tool. The Automatic Tie Point Collection Tool also required two manually selected tie points for each overlap area in the block of images. For example, the December 5, 1962 photography required that two common points be identified on image pairs 79 and 80, 80 and 81, 81 and 82, and 82 and 83. Thus, a total of 8 tie points for the block had to be selected. The Automatic Tie Point Collection Tool was then run, using the default values for the strategy parameters such as search size, correlation size, and least square size. The maximum number of points per image was set to be 50. The number of resulting tie points was dependent on photo quality and the amount of overlap, but was generally between 20 and 50 points per image pair. Choosing this many points manually would have been a prohibitively time-consuming process. All tie points were then inspected for error. The few erroneous points were deleted. In a few cases, an insufficient number of tie points were found, and additional points had to be chosen manually. Unless they were needed, the initial two points selected on each image pair were always deleted, with the assumption that computer generated tie points were more accurate than those chosen manually. Table 5-2 lists the number of tie points that were used on each image. This number reflects all manually chosen and computer generated points that were used in the final product. It should be noted that, due to a glossy finish on the 1972 photos, Imagine was unable to automatically generate tie points. In this case, between 5 and 8 tie points for each photo pair were chosen manually.

Table 5-2. Number of tie points per photo pair.

Photo Date	**Image Pair**	**Number of tie points**
March 14, 1962	128-130	48
	130-131	23
	131-132	18
	132-133	23
	133-134	6
	134-135	39
December 5, 1962	79-80	24
	80-81	21
	81-82	26
	82-83	9
	83-84	45
	84-85	30
November 6, 1972	136-137	8
	137-138	8
	138-139	5
	139-140	5
	140-141	5
	141-142	5
	142-143	5

Table 5-2. Number of tie points per photo pair.

Photo Date	Image Pair	Number of tie points
October 21, 1980	3874-3875	53
	3875-3876	9
	3876-3879	39
September 19, 1984	271-272	34
	272-273	17
	273-274	20
	274-275	37
October 1, 1986	63-64	41
	64-65	10
	65-66	18
	66-67	19
	67-68	28
	68-69	44
June 17, 1992	646-647	48
	647-648	18
	648-649	24
	649-650	23
	650-651	24
	651-652	23
	652-653	23
	653-654	26
	654-655	46

Once the tie points for a block were finalized, each image has been successfully referenced to the others in the block.

The next procedure was to georeference this tied strip of images to real world coordinates. Traditionally, there have been several variations on this process, each with differing levels of accuracy. Perhaps the most accurate method of identifying real world coordinates would be collecting and specifying GPS coordinates of visible landmarks. Modern aerial photography missions often distribute targets, shaped like Vs, on the ground throughout the study area. GPS coordinates are collected for these targets, which are visible on the photography. Within such controlled photographic missions, ground control points can purposely be placed anywhere they are needed. This allows for a distribution of points throughout the entire photographic area. While this method is ideal, such predetermined coordinates for ground locations do not generally exist for historical photography. Even recent photos frequently have become separated from the coordinates of the associated control points. In these cases, another method for establishing ground control is required. A basemap, with known coordinates, can be used to georeference the photography. Points on the historical photography are matched to the same landmarks seen on the basemap. These basemaps are frequently NOS T-sheets or USGS 1:24,000 quad sheets, due to their nationwide coverage. The use of these basemaps is subject to the error associated with identifying identical points on two different maps, as well as the uncertainty implicit in the basemap. For the quad sheets, whose accuracy is governed by NMAS, the maximum allowable error for 90% of the points is 40.0 feet [12.2 meters]. Additionally, there is almost always a discrepancy in dates between the quad sheets and photography, which results in further error if non-stable points, such as the estuarine shoreline or vegetation features, are used for control. Yet another drawback is that very few common points can be identified, due to the lack of detail on the quad sheets. For these reasons, even though USGS quad sheets were available for the study area, 1998 orthophotography was used as a basemap to establish ground control. These orthophotos, produced especially for North Carolina's erosion rate update, have a horizontal positional accuracy of 0.5 feet. This change in basemaps represented a significant improvement over the methodology used in the creation of the COAST database.

ERDAS Imagine provided a convenient interface for identifying ground control points, as shown in Figure 5-2. An historical photo was displayed on one side of the screen, and the appropriate 1998 orthophoto was displayed on the other. The user was able to zoom into the pixel level on each photo, and click to establish common points.

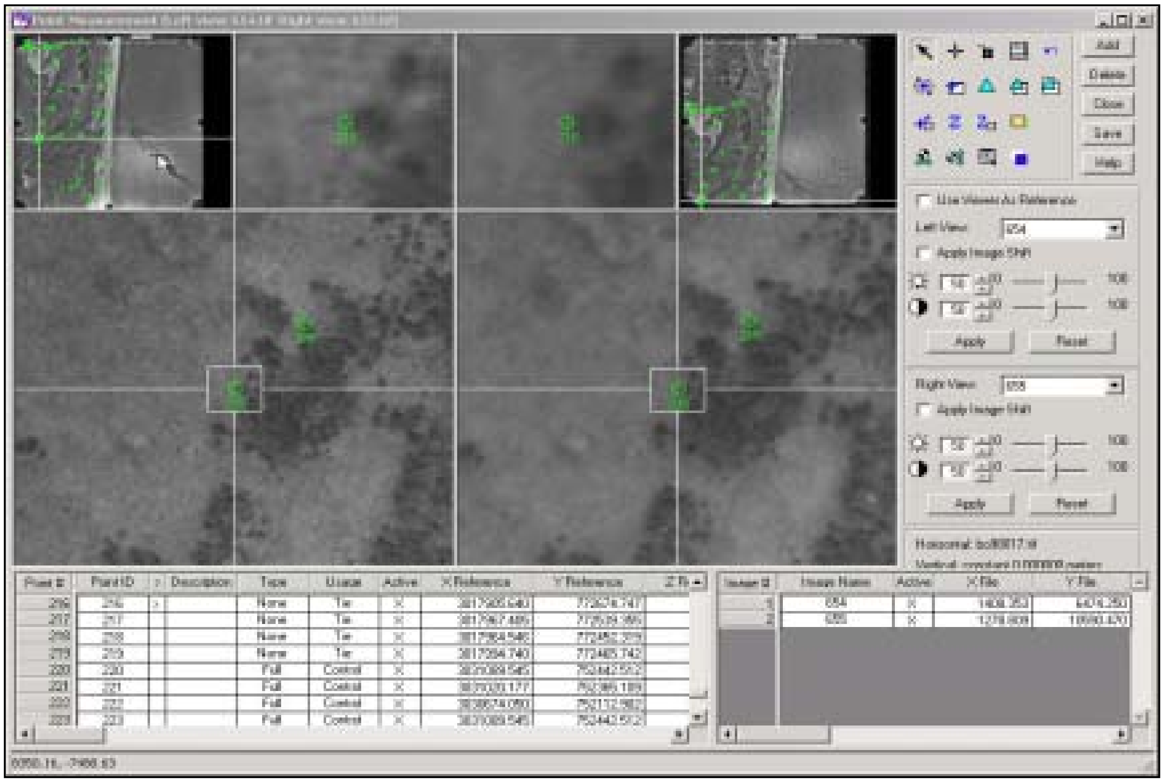

Figure 5-2. Point measurement window from ERDAS Imagine.

Suitable points for ground control included road intersections, piers, and corners of structures at ground elevation. In a few cases, when no other points were available, stable points on the estuarine shoreline were chosen. In all cases, only points at ground level were used. The use of rooftops, tops of telephone poles, or any other points with significant elevation would introduce error due to relief displacement, as discussed in Section 2-2. For obvious reasons, points were more plentiful in the recent photography than in the 1960s photography. ERDAS recommends choosing two ground control points (GCPs) for every third image in a strip of adjacent images. In this study, a significantly higher number of GCPs were used for each date. ERDAS also notes that the GCPs would ideally be evenly distributed across the photograph to accurately model the camera. Since most development in this study area occurs along a north-south highway, points chosen in each photo were usually evenly distributed in the north-south direction, but not necessarily from east to west. This would be cause for concern if the shoreline was consistently on the edge of the photos. However, since this is a narrow barrier island, there is a very small horizontal distance between the highway and the shoreline. Table A-1 lists coordinates and descriptions of all chosen ground control points. Each GCP must have a vertical elevation associated with it. Ideally, these elevations would be automatically extracted from a Digital Elevation Model (DEM). Since historical elevation data did not exist for the study area, all GCP elevations were set to zero. In an area with highly variable topography, this would be cause for concern. On a barrier island with all elevations less than about 10 feet, this likely introduced only a negligible amount of error (Gorman *et al.*, 1998; Stafford and Langfelder, 1971).

Once the GCPs and tie points were established, the software ran a block triangulation procedure and estimated the exterior orientation parameters for each image. Each image had 6 such parameters associated with it: x, y, and z (positional elements of the camera at the moment of photography); and omega, phi, and kappa (rotational elements of the camera at the moment of photography). Omega is the rotation around the photographic x-axis, phi is the rotation around the photographic y-axis, and kappa is the rotation around the photographic z-axis (ERDAS website, 2002). The identification of these exterior orientation parameters finalized the information that Imagine needed to complete the rectification procedure. Once a triangulation is accepted, a transformation equation is applied to each photograph. Each image then underwent a calibration, in order to save the absolute orientation information with each image. These calibrated images were then mosaicked into one, using the default cutlines provided by Imagine. The cell size, which must be specified for the resampled image, was left at the recommended value in order to avoid loss of data. At this point, the individual rectified images for a date have been combined into one nearly seamless image, which was referenced to real-world ground coordinates. This image was saved as an uncompressed TIFF 6.0 file, frequently over one gigabyte in size. Figure 5-3 is an example of a finished photo mosaic (September 19, 1984) and a close-up of the intersection of individual photographs within the mosaic. Photo mosaics with ground control points are included as Figures A-1 through A-7 in Appendix B. Within a mosaic, differences between the photos can be seen due to the change in wave and sun conditions, but the shoreline and other land features are continuous.

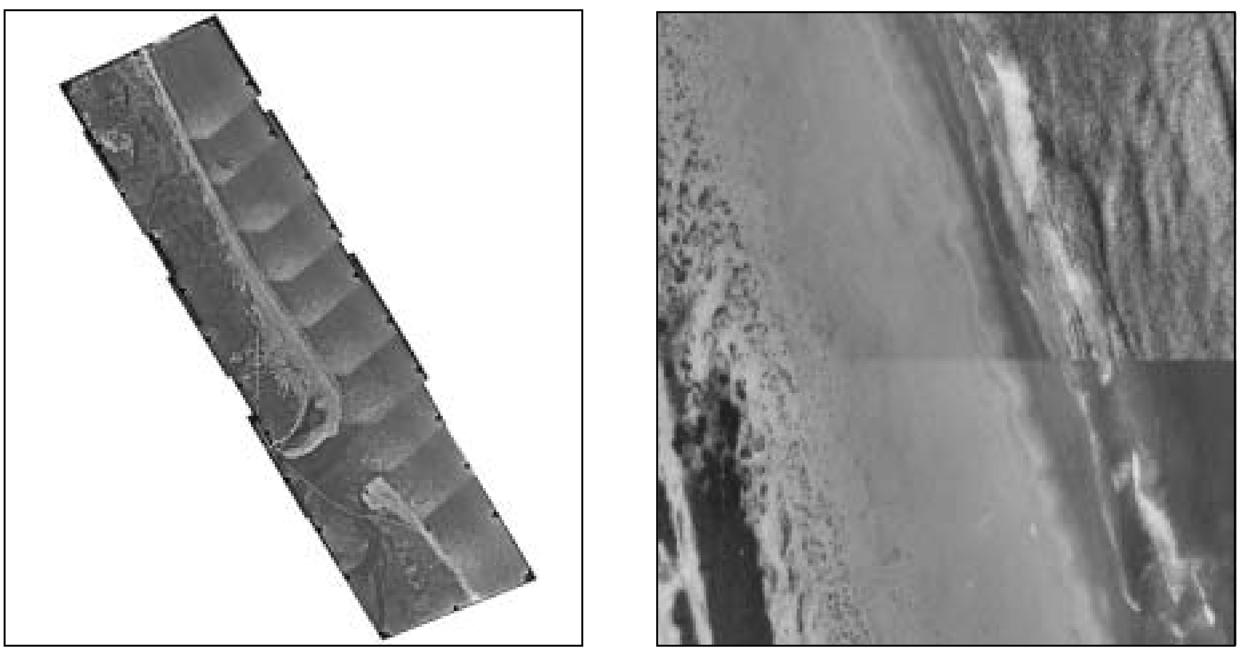

Figure 5-3. September 19, 1984 mosaic (left) and close-up of photo intersection (right).

5.2. Shoreline Identification

There are a number of possible features on the subaerial beach that can be interpreted as a shoreline. These include the swash terminus, mean low water, high water line, and berm line. In order to minimize the error associated with comparing shorelines of different dates, the same interpretation must be consistently applied. Three requirements have been identified that are essential for shoreline recognition on aerial photography (Doaln, 1978):

1) the shoreline must be easily and consistently recognizable
2) the shoreline must be linearly continuous
3) positional variations across the beach due to changes in water level must be at a minimum

Of nine possible shoreline interpretations listed by Dr. Dolan, only the high water line (HWL) meets all three criteria. The high water line is defined as the limit of variable wave runup on the beach slope (Langfelder *et al.*, 1970). However, without knowing the tide and wave conditions at the moment of photography for each study date, it was impossible to specifically delineate the high water line on the low quality photographs. For this reason, the wet/dry line was used as an approximation of the high water line. The wet/dry line is reestablished at each high tide based on the beach slope and the current wind and tide conditions (Dolan *et al.*, 1978). Thus, it actually represents a time average of the high water line (Overton and Fisher, 1996). The wet/dry line is seen on the aerial photograph as a change in color or gray tone, as illustrated in Figure 5-4.

Figure 5-4. Digitized wet/dry line.

This difference in gray tone is caused by differences in the water content of the sand on either side of the line (Langfelder *et al*., 1970). It has been shown that the wet/dry line closely approximates the HWL (Moore, 2000). All pre-existing shorelines used in this study (NOS T-sheets, COAST data) represented the high water line. For this reason, as data was created in this study, the wet/dry line was digitized as the shoreline.

The wet/dry line was digitized on each finished photo mosaic in ArcView 3.2. In accordance with the procedure used in North Carolina's 1998 erosion rate update, the shoreline was digitized mostly at a scale of 1:600, with zooming in and out taking place as needed.

5.3. Erosion Rate Calculation

There are a number of data analysis techniques that can be used to compute shoreline erosion rates. An informed decision on the technique used is essential, since the type of data analysis can be responsible for much of the potential variability in the calculation of rates (Crowell and Buckley, 1992). The most prevalent, an endpoint method of rate calculation (EP), is used by more than two-thirds of agencies that use shoreline data to manage coasts (Fenster and Dolan, 1994). This method computes a rate by simply taking the net difference between two shoreline positions and dividing it by the time interval between the dates of the two shorelines. The endpoint method has been shown to produce a highly variable prediction depending on which two shorelines are used (Honeycutt *et al.*, 2001). The North Carolina DCM is one of the agencies that uses rates found by the endpoint method for policymaking. Despite the availability of shorelines of several intermediate dates, the erosion rates used by the DCM have been computed solely from the earliest shoreline position in the COAST database and the current position (Benton *et al.*, 1997). Within this study area, for example, the official rate in the 1992 erosion rate update was calculated using shoreline positions from July 1, 1945 and June 17, 1992. A second method for calculating rates is through linear regression (LR). With linear regression, a line is fit to multiple shoreline positions that minimizes the sum of the squares of the differences between measured and calculated shoreline positions. Linear regression potentially reduces the impact of one or two anomalous values on the accuracy of the calculated rate (Honeycutt *et al.*, 2001). However, regression can be sensitive to uneven point distribution and point clusters (Foster and Savage, 1989). In order to ensure meaningful results, shorelines used in regression should be well distributed through time. Other rate calculation methods include jacknifing, an average of rates (developed by Foster and Savage, 1989), and a Minimum Description Length (MDL) (developed by Fenster *et al*., 1993). Since the EP and LR are the two primary methods used to calculate erosion rates, they were the only ones applied in this study.

Once shorelines were digitized for the seven aerial photography dates, all the shorelines necessary for this study were in ArcView shapefile format. Erosion rates were calculated using the method of shore-parallel baselines, as developed in the original OGMS. Though established baselines already existed for the entire state, three new baselines were drawn to be parallel to the shorelines specific to this study. At the southern end of the study area, the effect of Oregon Inlet has been to produce highly variable shoreline positions. As a result, it was impossible to draw a baseline that was parallel to all shorelines near the inlet. This must be considered when analyzing erosion rate data near the inlet. Transects were generated perpendicular to the baselines at intervals of 164 feet [50 meters]. This transect spacing was chosen to be consistent with the interval used in the generation of the COAST data. Transects were numbered from 1 to 298, with transect 1 at the north and transect 298 at Oregon Inlet. Due to variations in photo availability, all transects did not intersect a shoreline from every date. In reality, the northernmost extent of most of the shorelines analyzed in this study was around transect 100. It is important to note that area covered by basemap HAT36 from the OGMS is equivalent to transects 208-298 in this study. All COAST shorelines (except June 1992) demonstrate a significant discontinuity between basemaps HAT37 and HAT36, likely due to the lack of control points available for HAT36. This will be demonstrated in the following section. For this reason, data from study transects 208-298 was, at times, studied separately from transects 1-207. Once transects and all shorelines existed in digital format, an ArcView script was used to find the coordinates of all shoreline/transect intersections, seen in Figure 5-5.

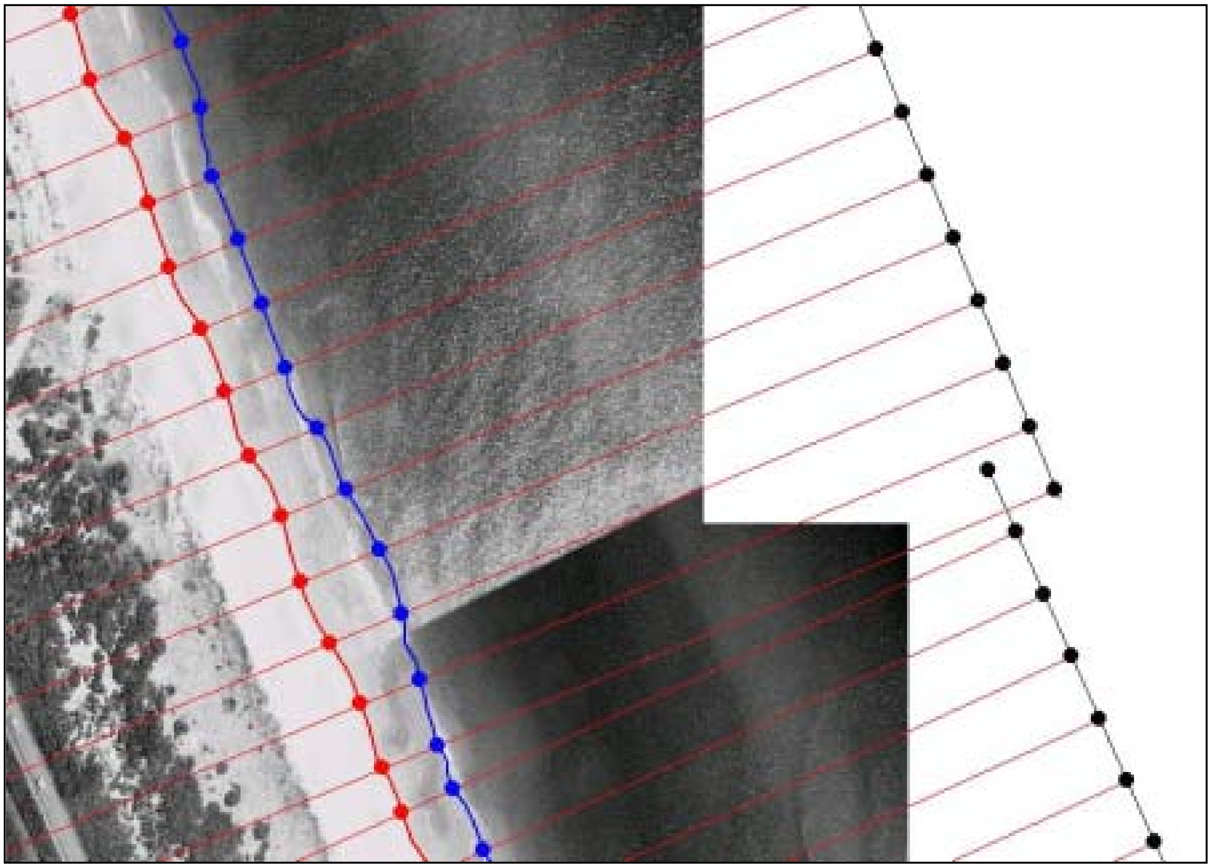

Figure 5-5. Intersection points of transects with baseline (black), December 1962 shoreline (blue), and June 1998 shoreline (red).

These coordinates, along with the coordinates of the transect/baseline intersections, were exported to a spreadsheet. The distance between shoreline and the baseline along all transects was then computed. Distances from baseline for all shorelines used in this study are included in Table A-2. Once the distances were known for each date and each transect, a variety of erosion rates were calculated. Rates were calculated using the endpoint method (EP) or linear regression (LR) for the combinations of shorelines presented in Table 6-3.

6. ANALYSIS

The numerical analysis conducted for this study was two-fold: First, each of the new shorelines was directly compared to the COAST shoreline of the same date. This demonstrated that the new shorelines were significantly different than the COAST shorelines, and that further study was necessary. The methods that were used in 1996 to create the 1992 shoreline were evaluated and compared with the methods used to create the 1992 shoreline in this study. This gave insight to the reasons that the newly created shorelines differ in position from the COAST shorelines. Finally, erosion rates were calculated using the procedures described in the previous section. This allowed for further comparison between COAST and new shorelines. This analysis also compared the endpoint method to linear regression and rates found with and without storm-influenced shorelines.

Prior to any analysis, it was necessary to quantify the possible error associated with each shoreline position. All shorelines that existed prior to this study already have an associated error, as described in previous sections. The error associated with the new shorelines has not yet been discussed. The block triangulation procedure in ERDAS Imagine reported a root mean squared (RMS) error for every block of photography. This RMS error represented any of the original photo errors that were not removed (some error due to lens distortion and relief displacement). An additional source of error was the basemap used for rectification. In this case, the basemap was 1998 orthophotography, with horizontal accuracy of 0.5 feet. In addition to the error associated with rectification of the historical photography, there was error associated with the interpretation of the shoreline position. Following a method developed by Moore and Griggs (2002), the interpreted shoreline position was assumed to lie within a circle (inscribing the area of a three pixel by three pixel square) of the true shoreline position. The sum of the two rectification errors (basemap and RMS) and the shoreline position error were both assumed to have an independent, bivariate normal distribution. These two errors were then summed under the RMS method. Table 6-1 quantifies the errors for each date of photography. The RMS error from rectification was the error reported by Imagine after triangulation. The summed rectification error is the rectification error plus the basemap uncertainty of 0.5 feet. As a conservative measure, the final uncertainty used in this study was defined as two times the RMS error. Thus, 95% of shoreline positions were expected to fall within the final uncertainty range of the true shoreline position.

Table 6-1. Quantification of uncertainty for study shorelines.

Date of shoreline	**RMS error from rectification**	**Summed rectification error**	**Shoreline interpretation error**	**Composite RMS error**	**Final uncertainty**
Mar 1962	8.85 feet	9.35 feet	1.41 feet	9.5 feet	18.9 feet
Dec 1962	4.42 feet	4.92 feet	0.71 feet	5.0 feet	9.9 feet
Nov 1972	4.13 feet	4.63 feet	1.41 feet	4.8 feet	9.7 feet
Oct 1980	1.79 feet	2.29 feet	1.41 feet	2.7 feet	5.4 feet
Sep 1984	1.03 feet	1.53 feet	2.82 feet	3.2 feet	6.4 feet
Oct 1986	1.10 feet	1.60 feet	1.41 feet	2.1 feet	4.3 feet
Jun 1992	1.30 feet	1.80 feet	1.41 feet	2.3 feet	4.6 feet

6.1. Comparison of Shoreline Positions

Each of the new shorelines was directly compared with the COAST shoreline of the same date. The difference in position along each transect was found for each of the seven pairs of shorelines. The COAST shoreline's distance from baseline was subtracted from the new shoreline's distance. Thus, negative differences occurred when the COAST shoreline was landward of the new shoreline, while positive differences occurred when the COAST shoreline was seaward of the new shoreline. On average, there were over 160 transects of data for each pair of shorelines. Each shoreline pair was analyzed on two levels: transects 117-207 and transects 208-298. Transect 117 was the northernmost for which data existed for all study shorelines. Transects 208-298 corresponded to basemap HAT36 from the COAST database. This basemap contained the southernmost area on the Bodie Island spit, and had a lack of features that could be used as ground control points. As a result, all the COAST shorelines (except June 1992) had a great discontinuity between HAT36 and the neighboring basemap, HAT37. As seen in Figure 6-1, shorelines shifted at least 500 feet landward as these basemaps changed. If transects 117-298 were solely analyzed as one group, results would have been skewed by the generally large difference between shorelines of the same date on the southern part of the island.

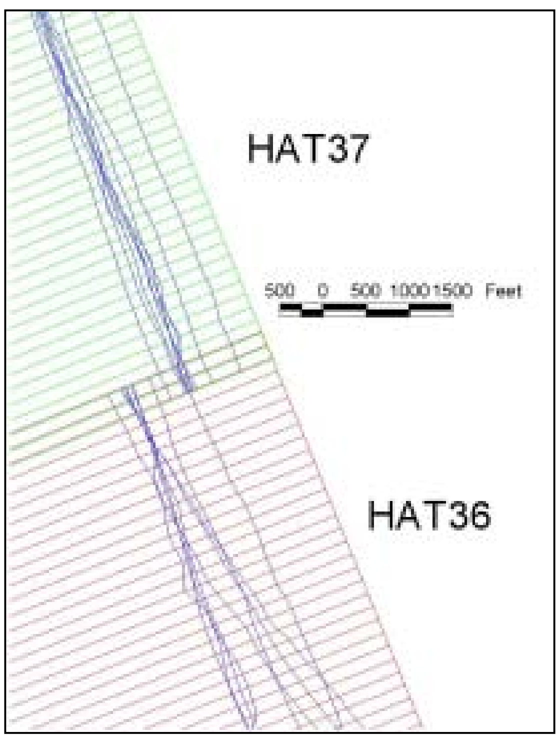

Figure 6-1. All COAST shorelines at intersection of basemaps HAT36 and HAT37.

The mean and standard deviation were found for the absolute differences between each shoreline pair. The new 1972 shoreline was not included in this comparison since the nearest COAST shoreline was from 1974. A maximum expected error was found for each pair by adding the 42.2 feet of uncertainty from the COAST position to the uncertainty from the new shoreline, as given in Table 6-1. The percentage of transects with positional differences greater than this expected maximum error was calculated. These results are summarized in Table 6-2.

Table 6-2. Comparison of COAST shorelines with new shorelines.

	Percentage of transects for which new shoreline is seaward of COAST shoreline	**Average of absolute differences (feet)**	**Maximum expected difference (feet)**	**Percentage of transects for which difference is greater than maximum expected**
March 1962				
117-207	79	58	61.1	45
208-298	100	762	61.1	100
December 1962				
117-207	90	45	52.1	43
208-298	100	560	52.1	100
October 1980				
117-207	4	54	47.6	56
208-298	no data	31	47.6	5
September 1984				
117-207	0	74	48.6	85
208-298	100	438	48.6	100
October 1986				
117-207	0	50	46.5	52
208-298	100	540	46.5	100
June 1992				
117-207	4	35	46.8	26
208-298	0	125	46.8	80

The first data column shows that, for transects 117-207, the two new 1962 shorelines were consistently seaward of the COAST shoreline of the same date. Conversely, for transects 117-207, the new shoreline for the latter four dates was consistently landward of the COAST shoreline. With the exception of 1992 (and 1980, which had no COAST shoreline for transects 208-298), the new shoreline was always seaward of the COAST shoreline near the inlet. There was a difference in shoreline position greater than the expected maximum error for over 50% of the transects between 117 and 207. This was the case for nearly all of the transects south of number 207. The October 1980 shorelines appeared to be an exception, but this was due to the majority of the HAT36 COAST data missing for this date. The COAST version of the June 1992 shoreline was created using different methods than all previous COAST shorelines. This resulted in a much smaller discontinuity between basemaps HAT36 and HAT37, as well as a smaller than usual discrepancy between the two 1992 shorelines. In all cases, including 1992, there was a significant difference between the compared shorelines. Further study is warranted to determine which of these shorelines should be taken to be more accurate.

6.2. Comparison of Methods

The 1992 erosion rate update, which included establishing the position of the 1992 shoreline, was completed in August 1997. Hence, there still exists documentation of the entire process used in the mid-1990s, hereafter referred to as the “old” procedure. The procedure from this study, the “new” procedure, used the same photography as was used in the old procedure. The comparison between the two procedures provided insight as to the advantages inherent in digital photogrammetric methods.

The photos used in the 1992 update were taken by the Photogrammetry Unit of NCDOT. For the state, a set of 750 mylar prints was produced at a scale of 1:4800. Dr. Robert Dolan then interpreted the wet/dry line and the vegetation line on each print. Prints were produced with 60 percent overlap, so only the centers of each print were used. 7 ½ minute USGS maps at a scale of 1:24,000 were used for control. Points which were visible on both the USGS map and the mylar print were chosen as ground control. Efforts were made to preferentially choose cultural features over natural features when possible. Point features were chosen to be of low relief and to be well-dispersed throughout the photograph. The USGS maps were then taped to a digitizing tablet. Points of known latitude and longitude, as well as control points, were digitized from the USGS map. This established a set of digital control points with known coordinates. The same locations were digitized on the mylar prints. The computer software then performed a technique known as rubbersheeting, in which each print was mathematically stretched to align the control points from ground and object space. Thus, a new coordinate system was established for each print, with the intent of reducing errors due to distortion and scale difference. The shoreline and was digitized into a latitude/longitude coordinate system (Benton *et al.*, 1997).

The notable differences between the old and new methods of photo correction are summarized below:

- Basemaps: USGS map (old); recent orthophotography (new)
- Tie points: none (old); multiple computer generated (new)
- Control points: mostly natural features (old); mostly cultural features (new)
- Photo correction technique: rubbersheeting (old); camera position modeling (new)
- Shoreline delineation: drawn at scale of 1:4800 (old); 1:600 (new)

As discussed in Section 4, the accuracy of USGS maps is governed by NMAS. For the 1:24,000 basemaps used in the old procedure, 90% of the points must be within 40.0 feet [12.2 meters] of their true location. For the 1998 orthophotography, the uncertainty was defined as 0.5 feet. Since a delineated shoreline can only be as accurate as the basemaps used to find it, this change in basemaps represented a significant improvement in horizontal accuracy. Additionally, the USGS map for this study area (named Oregon Inlet, N.C.) was originally drawn in 1953, then photorevised in 1983. It is likely that more point features could be matched between 1992 and 1998 than between 1992 and 1983.

Within the new procedure, several tie points were generated for each photo, as described in Section 5.1. The old procedure had no points designated solely as tie points. The luxury of tie points did not practically exist in an analog setting. The old procedure did identify some of the same points for ground control on overlapping photographs. In this way, up to four points on some of the photo pairs served as tie points. These few points likely went a long way toward eliminating discontinuities between shorelines from neighboring photos, but certainly did not provide the benefits seen from the 201 precisely chosen tie points in the new procedure.

Records exist of the specific control points used in the mid-1990s. Both their coordinates and a written description of each point have been preserved. Descriptions of points used in both procedures are listed in Table A-1. From this table, it can be seen that the old study measured 35 distinct GCPs for the study area, as opposed to the 20 used in the new study. However, of the 35; 16 were considered cultural features and 19 were natural (all marsh features). Of the 20 new points, only 3 were natural features. The relative abundance of possible control points in the 1998 orthophotography allowed the user to choose only those of the highest quality. In addition to being able to choose points with higher accuracy, the points could also be measured with a higher degree of precision. Within the old procedure, points were marked on a 1:24,000 map. The new procedure allowed the user to zoom in to the individual pixels on the screen. Depending on the pixel size (see Table 5-1), points could be measured to within 1 to 2 feet of their location on the photo. Figure 6-2 shows a ground control point from the old study. It is first shown with a background of the USGS quad sheet at the scale of the paper map. The second illustration is a zoomed-in representation of the first. The red point represents the digitized ground control point. The detail seen in the second image was not available when the points were initially measured. In retrospect, it can be seen that this point was digitized about 20 feet away from its intended map location, which was the tip of the nearby land protrusion, colored in black. It was not unusual to find similar error upon the inspection of the remainder of old ground control points.

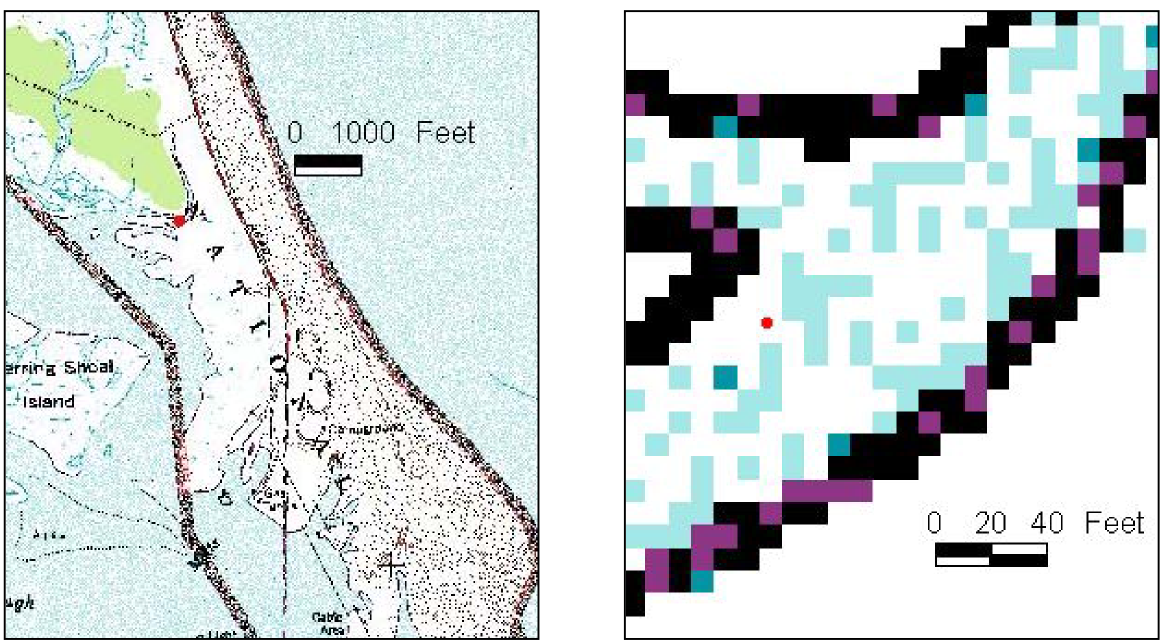

Figure 6-2. USGS quad sheet with GCP from "old" rectification procedure.

Of additional concern was the mathematical method used in the rectification of the photos. As described above, the old study made use of a technique referred to as rubbersheeting, where, using a computer program, the image was linearly stretched to fit it to the digitized control points (Benton *et al.*, 1997). As mentioned in Section 2.2, the rubbersheeting procedure can correct for scale variations, but does not fully account for errors due to tilt or lens distortion. These latter two types of distortion are not linear in nature, and cannot be corrected for by simply stretching a photograph. Distortion due to 3 degrees of camera tilt was previously shown to result in over 60 feet of horizontal error. While the camera used for the 1992 photography was likely of high enough quality to avoid such extreme tilt, several feet of tilt-related error were still to be expected. The transformation used by ERDAS Imagine used the ground control points to model the pitch, yaw, and roll of the camera at the moment of photography. Thus, the effect of tilt was quantified and subsequently removed. It should be noted that lens distortion cannot be completely accounted for without knowing the exact model of camera used in the photography. As a result, the maps resulting from both old and new methods are susceptible to error from lens distortion.

Notwithstanding the photogrammetric processes, the method of shoreline delineation could have greatly affected the final shoreline position. In the old study, the shoreline was manually drawn on the mylar prints at a 1:4800 scale. This line, after rubbersheeting, was digitized. In this process, accuracy was compromised in two ways. First, operator error was introduced, since the person digitizing the line was not the person who initially interpreted the line. Secondly, in these cases, there was always an error associated with the width of the pen used to demarcate the line. If a 0.1 inch [0.3 mm] diameter pen was used to draw the wet/dry line, the resulting line had a thickness of over 4 feet. This error was a result of the scale at which the shoreline was drawn. This scale also affected the precision of the wet/dry line, as seen in Figure 6-3.

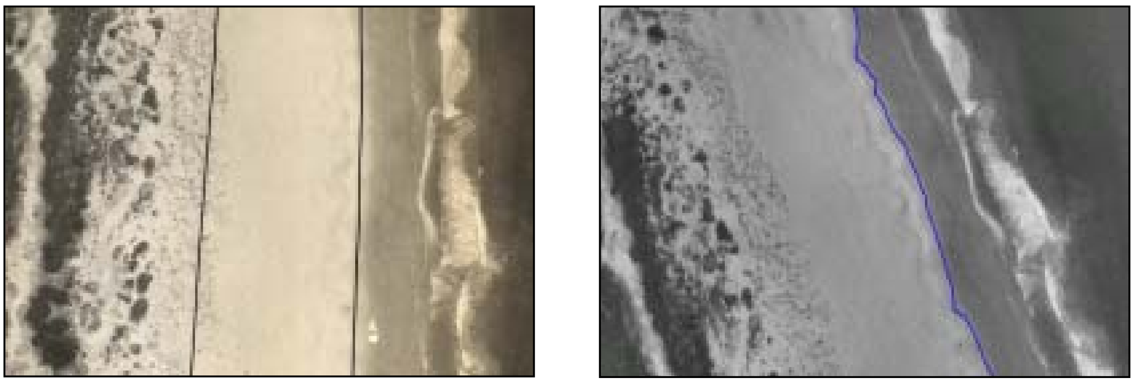

Figure 6-3. Comparison of shoreline delineation methods.

The old 1992 shoreline was drawn at a scale of 1:4800, while the new 1992 shoreline was drawn at varying scales. The image on the left is a scanned portion of the original mylar print on which the shoreline was drawn. The image on the right is of the same area, but with the new digitized shoreline overlaid on the new photo mosaic. It can be seen that the old wet/dry line was drawn with a lack of precision, due to the small scale. The new wet/dry line was drawn at the scale where individual pixels were visible.

It is difficult to quantify the maximum expected difference between the old and new 1992 shorelines. Any estimate should include the five differences in mapping techniques described above. Adding the maximum likely possible difference for each of the five differences yields a value of 85 feet (40 feet from basemap, no quantifiable difference from tie points, 20 feet from GCPs, 20 feet from photogrammetric procedure assuming one degree tilt, 5 feet from shoreline delineation). Statistically, this number of 85 feet means very little.

However, it would be accurate to say that any difference in 1992 shoreline positions of less that 85 feet could possibly be explained by these differences in procedure. This would account for differences in position at nearly all of the study transects.

6.3. Comparison of Erosion Rates

Table 6-3 lists all of the erosion rates that were calculated for analysis. These fourteen rates at each study transect are recorded in Appendix D.

Table 6-3. Descriptions of calculated erosion rates

Rate #	Calculation method	Dates used (T=T-sheet, C=COAST, N=new)
1	Endpoint	45C, 98
2	Endpoint	49T, 98
3	Linear Regression	Mar62C, Dec62C, 80C, 84C, 86C
4	Linear Regression	Mar62N, Dec62N, 80N, 84N, 86N
5	Linear Regression	Mar62C, Dec62C, 80C, 84C, 86C, 92C
6	Linear Regression	Mar62N, Dec62N, 80N, 84N, 86N, 92N
7	Linear Regression	Mar62C, Dec62C, 80C, 84C, 86C, 92C, 98
8	Linear Regression	Mar62N, Dec62N, 80N, 84N, 86N, 92N, 98
9	Linear Regression	45C, Mar62C, Dec62C, 80C, 84C, 86C, 92C, 98
10	Linear Regression	49T, Mar62N, Dec62N, 80N, 84N, 86N, 92N, 98
11	Linear Regression	45C, 80C, 86C, 92C, 98
12	Linear Regression	49T, 80N, 86N, 92N, 98
13	Linear Regression	All 11 COAST dates (45-92), 98
14	Linear Regression	49T, Mar62N, Dec62N, 72N, 80N, 84N, 86N, 92N,98

The combinations of dates used in the rate calculations were chosen with specific comparisons in mind.

Rate 4 was calculated using the five new shorelines that corresponded to existing COAST shorelines of the same date. Rate 3 was found using these five COAST shorelines. Therefore, a comparison between Rate 3 and Rate 4 indicated whether the shorelines

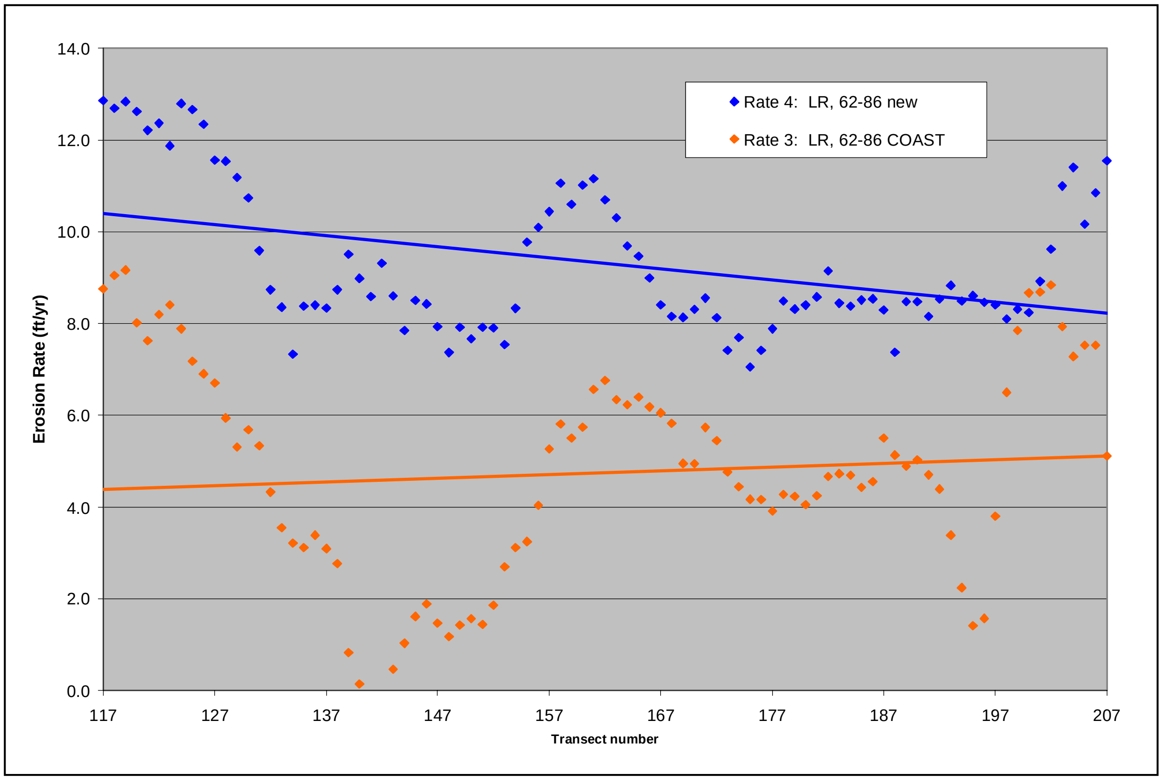

Figure 6-4. Rates 3 and 4 for study transects.

created in this study produced a significantly different rate than would have been calculated before this study. Although a 1972 shoreline was created in this study, it was not included in these two rate calculations since the nearest COAST shoreline date was in 1974. Rates 3 and 4 are plotted below in Figure 6-4, with linear trendlines included. The plot indicates that the rate using the new shorelines produced a rate consistently 4 ft/yr greater than the rate calculated with the COAST shorelines. It is not unexpected that the rates are different, but the fact that they consistently differ by approximately 4 ft/yr bears further investigation. The shoreline positions over time were plotted for transect 157, which appeared to be representative of all study transects. Figure 6-5 contains shoreline positions at transect 157 for the five COAST and the five new shorelines. The linear regression line was plotted for each. The slope of the plotted linear regression line represented the erosion rate at transect

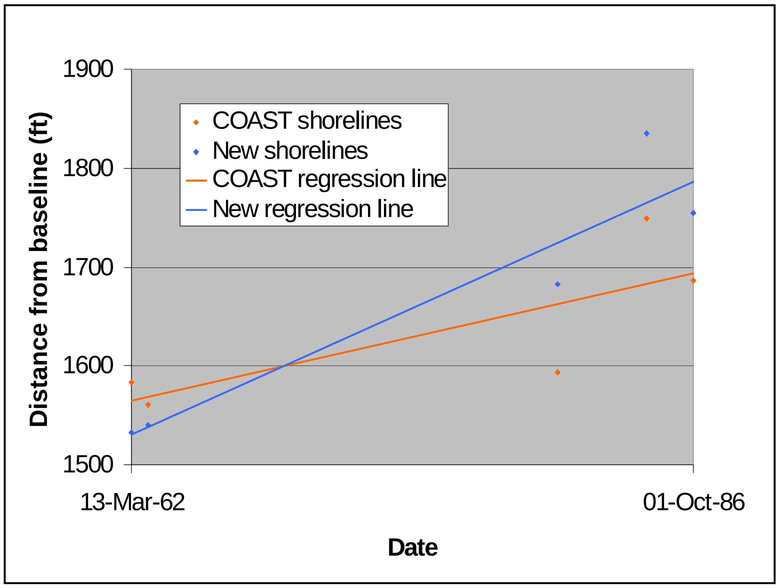

Figure 6-5. Linear regression lines for Rates 3 and 4 at transect 157.

157. At this transect, the erosion rate for the COAST shorelines was 5.3 ft/yr, and the rate for the new shorelines was 10.4 ft/yr. This difference in regression slopes is apparent in the above plot. It was clear that there was a positional difference in the shorelines for each of the five dates. If the COAST shorelines were consistently the same distance seaward of the new shorelines, as with the three more recent dates, then the erosion rates would be identical. However, at transect 157, COAST shorelines were landward of new shorelines for the two 1962 shorelines and seaward of the new shorelines for the 1980, 1984, and 1986 dates. This resulted in a significantly different erosion rate between the two sets of shorelines. For the entirety of the study area, it was generally the case that the new shorelines were uniformly seaward of the COAST shorelines for the 1962 dates, and uniformly landward of the COAST positions for the latter three dates. From a procedural point of view, it is unknown why this was the case. This constant spatial trend resulted in a difference between Rate 3 and Rate 4 which was nearly constant over the study area.

Rate 5 used the same shoreline positions as Rate 3, with the addition of the old 1992 shoreline. Likewise, Rate 6 used the same positions as Rate 4, with the addition of the new 1992 shoreline. Figure 6-6 is a plot of Rates 5 and 6 for the study transects. Much like the previous rate comparison, Rate 5 was consistently around 3 ft/yr less than Rate 6 across all study transects. The inclusion of the 1992 data caused the difference between the two rates to not be as great as the difference between Rates 3 and 4. As seen in Table 6-2, the positional difference in the two 1992 shorelines was substantially less that any of the other shoreline pairs. Figure 6-7 is a plot similar to Figure 6-5, but with the inclusion of the 1992 positions. At transect 157, Rate 5 was 5.9 ft/yr and Rate 6 was 9.0 ft/yr. The similarity between the two 1992 shoreline positions had a moderating effect on the difference between

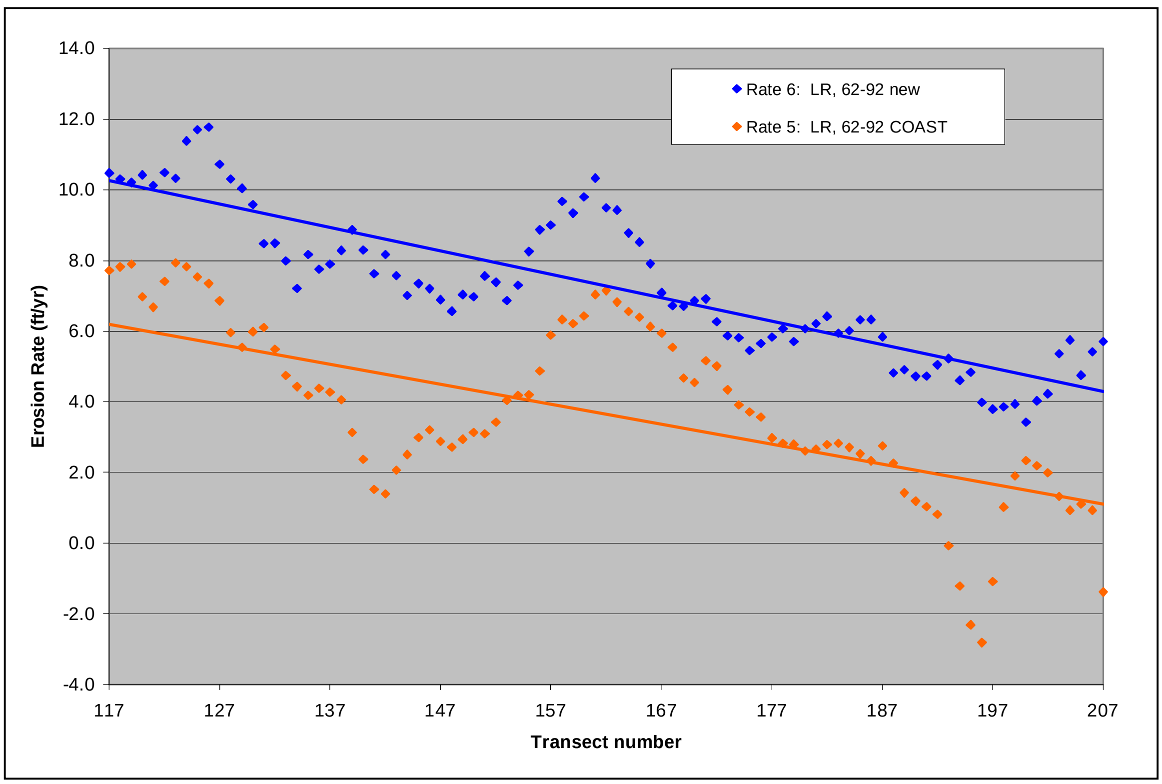

Figure 6-6. Rates 5 and 6 for study transects.

the two rates. Throughout the entire study area, the new 1992 shoreline was generally landward of the old 1992 shoreline. The difference was so slight, in comparison to differences between other shoreline pairs, that Rates 5 and 6 were effectively calculated using a common 1992 shoreline point.

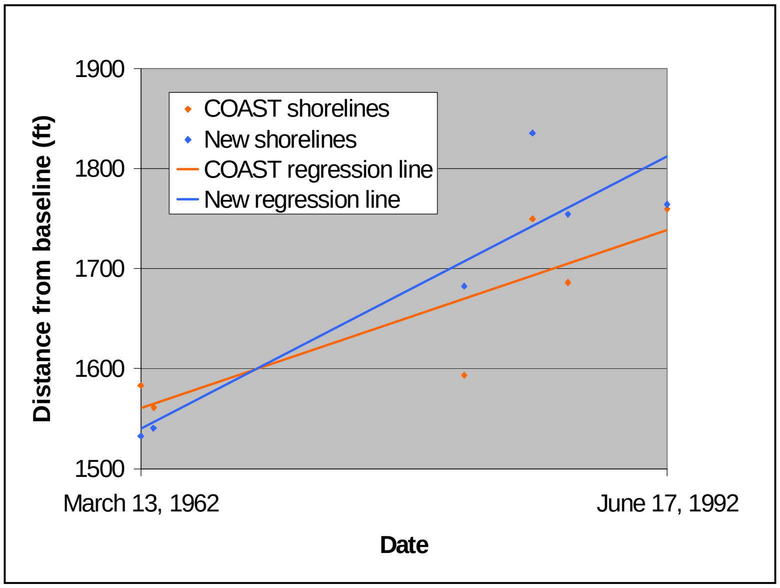

Figure 6-7. Linear regression lines for Rates 5 and 6 at transect 157.

The comparison between Rates 7 and 8 is also meaningful. Rate 7 was generated using the same COAST shorelines as Rate 5, with the shoreline from 1998 orthophotography included. Similarly, Rate 8 used the new shorelines from Rate 6, with the inclusion of the 1998 shoreline. The most recent shoreline position used in the calculation of Rates 7 and 8 was identical, since there was only one 1998 shoreline. Based on the results from the previous comparison, the expected result was that the two rates would differ by a constant amount, less than 3 ft/yr, over all study transects. This was indeed the case. As seen before, Rate 7 showed the same spatial trends as Rate 8. Rate 7 was consistently about 2 ft/yr less than Rate 8. The use of the same 1998 shoreline and the nearly identical 1992 shoreline positions effectively provided identical points for 1992 and 1998 in the Rate 7 and 8 regression calculations. As more modern dates were included in rate calculations, the slopes of the regression lines became more similar.

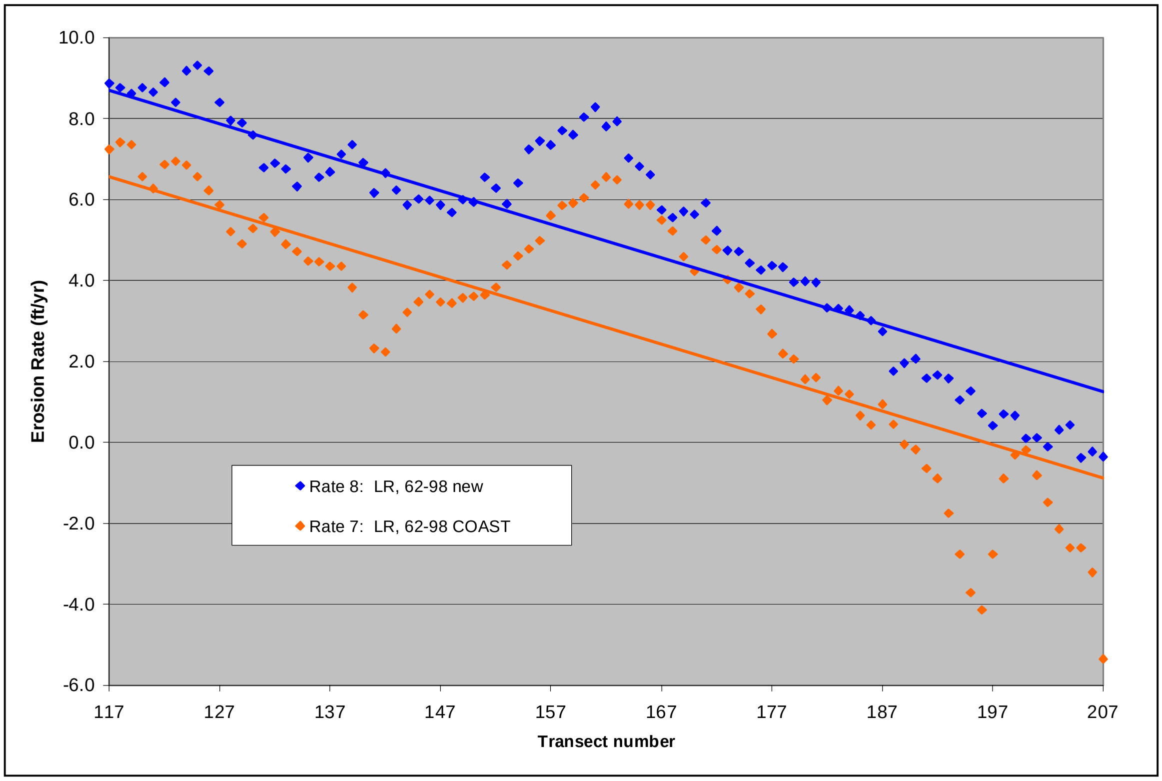

Figure 6-8. Rates 7 and 8 for study transects.

Rates 9 and 10 represented the same dates as 7 and 8, with the addition of the 1949 T-sheet and the 1945 COAST shorelines, respectively. Each of these rates represented a linear regression of shoreline positions from the 1940s through 1998. These two rates, and the next few that will be presented, are of utmost practical importance. If the North Carolina Division of Coastal Management ever chose to calculate an official erosion rate using linear regression, it would undoubtedly include shoreline positions dating to the 1940s. Rates 3 through 8, which have had 1962 as an early date, allowed for meaningful conclusions in this study, but did not span enough time to qualify as a long-term erosion rate. Rate 9 had the 1945 COAST shoreline as an early date. Ideally, this rate would be compared to one with an early shoreline position measured from newly rectified 1945 photography. Since such a shoreline was not available, the 1949 T-sheet was used as the early shoreline date in the Rate 10 calculation. DCM preferred the T-sheet over the early COAST date for use in the 1998 erosion rate update. For this reason, the T-sheet was used with the new shoreline data. Figure 6-9 compares Rates 9 and 10 over all study transects. It can be seen that the addition of the early date made this pair of rates the most similar of any presented so far.

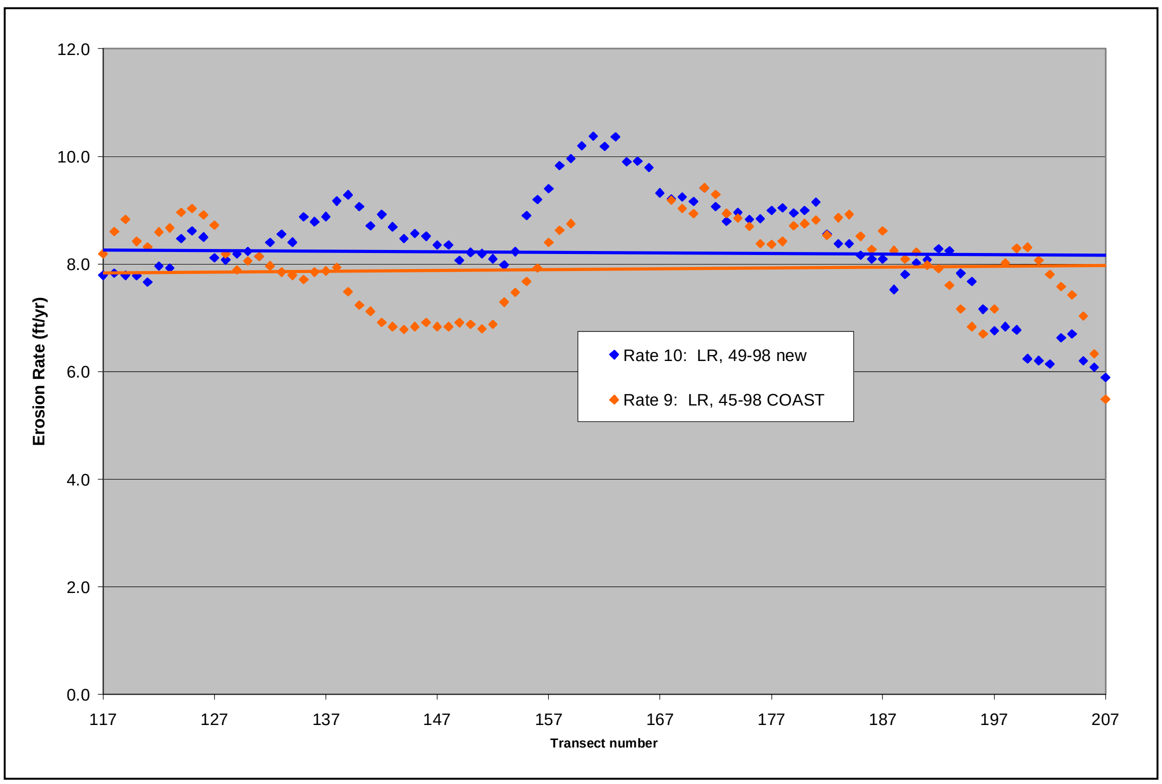

Figure 6-9. Rates 9 and 10 for study transects.

The rates differed by a maximum of 2 ft/yr, but were often effectively identical. Note that Rate 9 did not exist from transects 160 through 167, due to missing 1945 COAST data. The similarity of rates suggested that the 1945 and 1949 shoreline positions were quite similar. Indeed, when shoreline positions were plotted for transect 157, the two positions were found to be very similar. This can be seen in Figure 6-10. It must be noted that four years have elapsed, so the shoreline positions were not expected to be precisely the same.

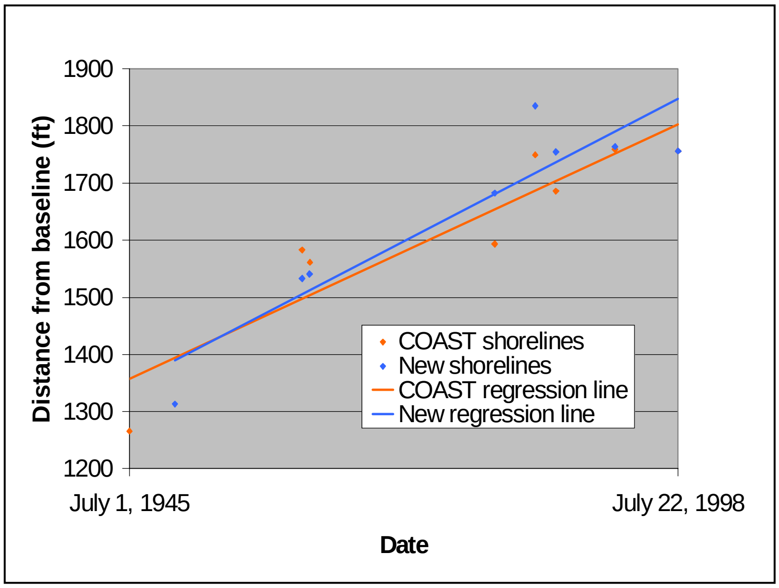

Figure 6-10. Linear regression lines for Rates 9 and 10 at transect 157.

Rates 11 and 12 were equivalent to Rates 9 and 10 calculated without the three post-storm shoreline positions. The comparison of Rate 9 with 11, and 10 with 12, showed the effects of removing the storm-influenced shorelines from the regression analysis. Per Table 3-1, the three storm-influenced shorelines in the set of dates for Rates 9 and 10 were March 1962, December 1962, and September 1984. According to Figure 6-10, these three shoreline positions were all landward of the positions predicted by Rates 9 and 10, reflecting post-storm erosion. Though there was no storm immediately prior to December 1962, this shoreline is still deemed post-storm, since it showed characteristics of a shoreline recovering from the massive Ash Wednesday storm. As shown in Figure 6-11, the absence of these

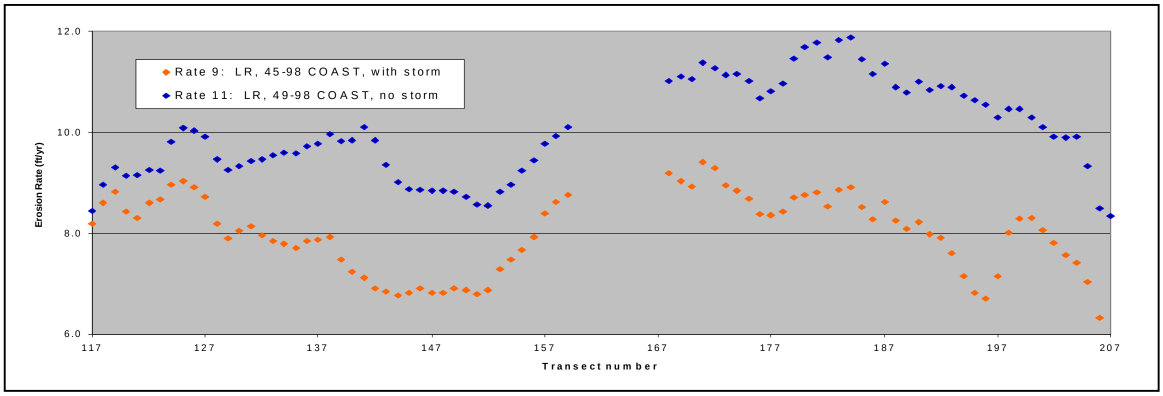

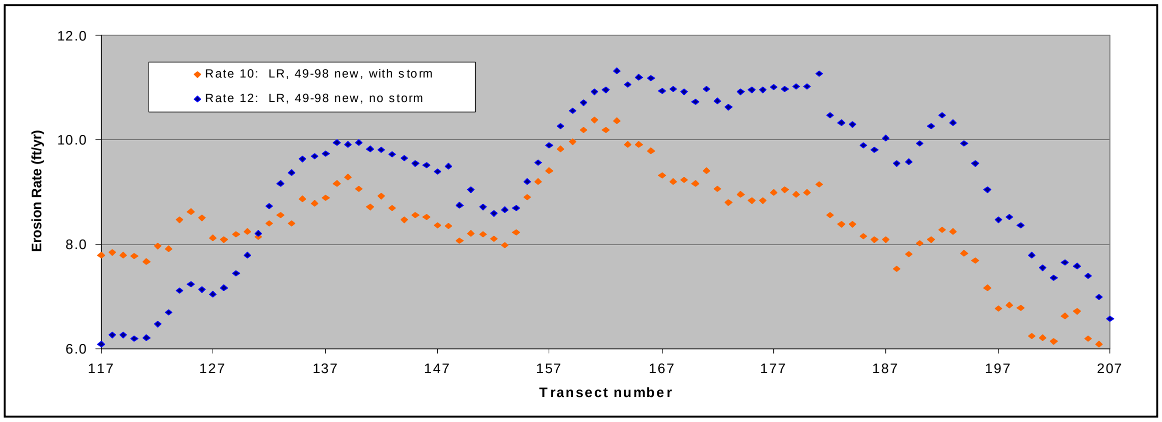

Figure 6-11. Rates 11 and 12 (no post-storm data) compared
with Rates 9 and 10 (with post-storm data).

three shorelines from Rates 9 and 10 resulted in, on average, close to a 2 ft/yr increase in erosion rate. This suggested that the inclusion of post-storm shorelines in regression analysis could noticeably change the resulting erosion rate. The rate did change, though not as severely, if post-storm shorelines were selectively included. For example, simply removing the March 1962 position from Rates 9 and 10 resulted in about a 0.5 ft/yr change in rates. For a more complete discussion on the impacts of including post-storm shorelines in rate calculations, refer to Fenster *et al*. (2001) and Honeycutt *et al*. (2001). Fenster *et al*. contend that the exclusion of post-storm shoreline data leads to a higher uncertainty in erosion rates, while Honeycutt *et al.* argue the opposite case.

The final rate comparison was perhaps the most important from a policy-making point of view. Rate 13 was calculated using the 1998 shoreline and all available COAST shorelines for the study area, as listed in Section 4.2. This represented a possible rate that would be used if DCM decided to compute an official rate using linear regression. Rate 14 was composed of all seven shorelines generated in this study, as well as the 1949 T-sheet and 1998 shoreline. This rate represented the best estimate of the true erosion rate for the study area, based on work done in this project. These two rates were also compared to Rates 1 and 2, which were both calculated using the endpoint method. Rate 2 was the official erosion rate used in the 1998 erosion rate update. Rate 1 employed the method used in the 1992 erosion rate update. Figure 6-12 shows Rates 13, 14, 1, and 2 plotted for all study transects. Rates 13 and 14 were exceptionally similar throughout the study area. The difference between the two was frequently negligible, and only exceeded 1 ft/yr for a few transects at the southern end of the study area. If both of these rates were to undergo the smoothing and blocking processes used by DCM to establish setback regulations, the rates would be identical for most of the study area. Rate 2, which represented the rate currently proposed for legislation, was within 1 ft/yr of Rates 13 and 14 for about half of the study transects. At the northern and southern ends of the study area, this endpoint rate diverged

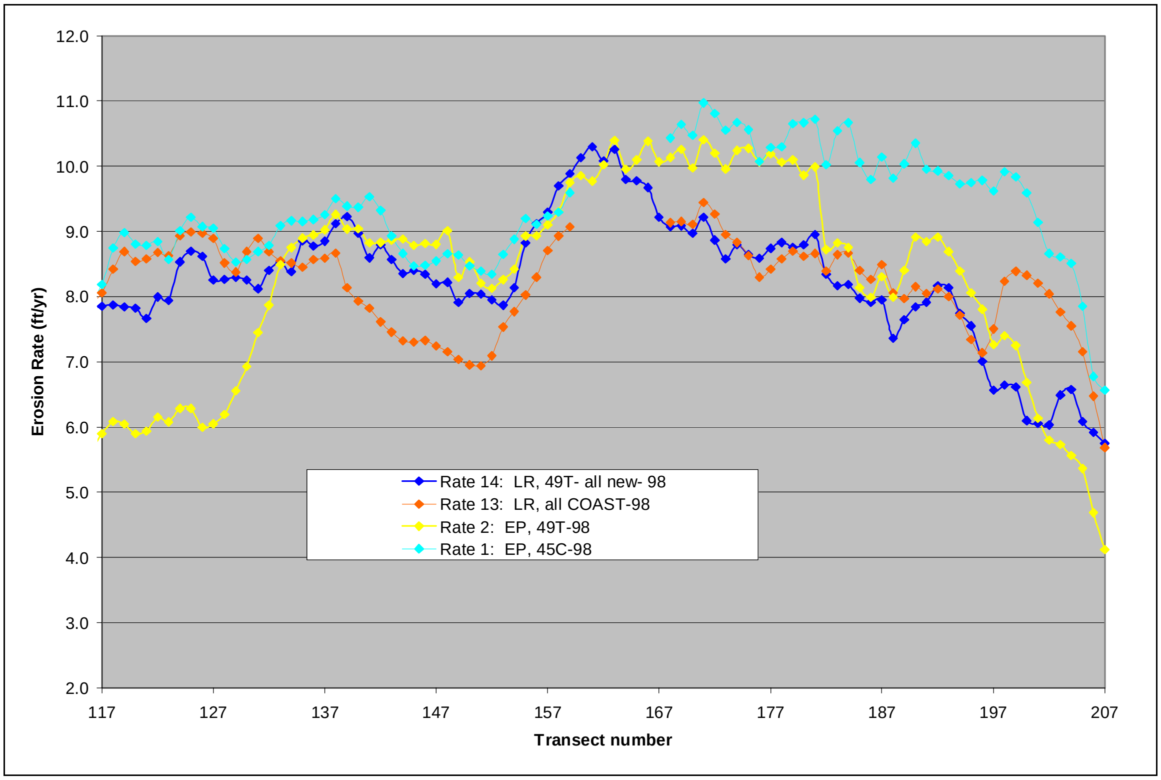

Figure 6-12. Rates 1, 2, 13, and 14 for study transects.

significantly from the regression rates. Rate 1 closely corresponded to the regression rates for the northern half of the study area. Another meaningful comparison was between the two endpoint rates. The difference between Rates 1 and 2 in the northernmost 15 transects was significant, but unexplainable. The difference between these two rates in the southernmost transects was likely due to effects of Oregon Inlet. In the 1940s, the inlet was located north of its current location, and could easily have caused significant shoreline erosion for the southernmost study transects between 1945 and 1949. This would explain the difference between the two endpoint rates in this area.

Table 6-4 summarizes the comparisons of erosion rates. The first pair of erosion rates compared a linear regression rate found with five of the new shorelines to the regression rate found with the COAST shorelines of the same dates. These rates were found to differ greatly. As more and more shoreline data was included in the regression calculations, the rates became more similar.

Table 6-4. Summary of erosion rate comparisons.

Rate Comparison	Mean absolute difference between rates (ft/yr)	Maximum difference between rates (ft/yr)	Notes
3: LR, 5 COAST dates 4: LR, 5 new dates	4.6	9.7	Rate 3 consistently lower than Rate 4; similar spatial trends
5: LR, Rate 3 + 1992 6: LR, Rate 4 + 1992	3.5	7.1	Rate 5 consistently lower than Rate 6; similar spatial trends
7: LR, Rate 5 + 1998 8: LR, Rate 6 + 1998	2.1	5.0	Rate 7 consistently lower than Rate 8; similar spatial trends
9: LR, Rate 7 + 1945 10: LR, Rate 8 + 1949	0.8	2.1	Nearly identical rates; less spatial similarity than previous comparisons
13: LR, 11 COAST dates + 1998 14: LR, 7 new dates + 1949, 1998	0.6	2.2	Nearly identical rates, with few exceptions
1: EP, 1945 (COAST), 1998 13: LR, 11 COAST dates + 1998	1.2	2.6	Clear difference between rates; different spatial trends
2: EP, 1949 (T-sheet), 1998 14: LR, 7 new dates + 1949, 1998	0.8	2.6	Clear difference between rates; different spatial trends
9: LR, Rate 7 + 1945 11: LR, Rate 9 without 3 storm dates	2.1	3.8	Rate 9 consistently lower than Rate 11; similar spatial trends
10: LR, Rate 8 + 1949 12: LR, Rate 10 without 3 storm dates	1.3	2.2	Rate 10 usually lower than Rate 12; less spatial similarity than previous comparison

7. RECOMMENDATIONS FOR FUTURE RESEARCH

The ideas and data presented in this study can be extended in a number of different ways. The photogrammetric procedure established through this study appears to be sound. There is likely little further research that needs to be done regarding the procedure. However, it should be applied to more shoreline dates and locations before strong assertions are made concerning the superiority of the technique. This study used seven dates of photography, of which six corresponded to dates used in the COAST database. There are eleven shorelines for Bodie Island in the COAST database. This leaves five existing sets of photography that could be rectified for this area. Specifically, the July 1, 1945 photos were not included in this study. A future study could include the 1945 photos and others to make a more exhaustive comparison of linear regression rates found using COAST and new shorelines. Additionally, several dozen modern digital shorelines (through a current NCDOT project) exist for this study area. These could also be included in regression analysis.

This entire study could also be replicated for another location on the coast of North Carolina. It would be interesting to see if the trends seen in the shoreline position comparisons occurred in other locations. A true picture of the worth of the COAST shorelines would start to appear if this study was repeated in areas away from inlets and in populated areas.

There are a few factors influencing erosion rates which were mentioned in this research, but were largely beyond the scope of this study. These include the rate calculation method and the inclusion of storm-influenced shorelines in regression analysis. As mentioned in Section 5.3, there exist a number of rate calculation techniques other than linear regression and the endpoint method. Additional methods could be considered in future study. Also, significant statistical analysis could be made concerning the worth of including post-storm shorelines. This is a subject for which there is no definitive answer in current literature.

Much progress could be made toward the understanding of uncertainty of shorelines and the corresponding erosion rates. It was fairly easy to quantify uncertainty for all shorelines in this study. When rates were calculated using the endpoint method, it was fairly easy to understand how to quantify the possible error in the rate. However, concerning linear regression, no shoreline studies in the current literature address the propagation of positional uncertainty through a linear regression rate calculation. All regression studies assume that the error in the rate is determined by the goodness of fit of the regression line. This does not account for errors that may be inherent in the shoreline positions.

Finally, it should be noted that no conclusions were drawn as to which set of shorelines is more accurate. Analysis was done to compare positions and rates of shorelines of the same date, but no claims were made as to which shoreline was more correct. It would seem that the COAST shorelines are inferior in accuracy to the newly generated shorelines, but this is difficult to prove. Future work could use various erosion rates to predict shoreline positions. Accuracy claims could then be made by comparing predicted positions to actual shoreline positions.

ERDAS Imagine can also be applied to coastal work other than shoreline erosion studies. DCM and North Carolina State University are currently using the procedures developed in this research to study inlet migration within North Carolina.

8. SUMMARY AND CONCLUSIONS

This study has demonstrated a new technique for the rectification of aerial photography. When applied to historical photography, the resulting shoreline positions differed significantly from previously accepted shoreline positions. The calculation of specific erosion rates accentuated the differences between the previously accepted and the newly rectified shorelines. However, when the comparison of erosion rates was studied from the point of view of a legislating agency, the differences became less significant.

In summary, seven sets of historical photography were acquired for Bodie Island, North Carolina. Most dates corresponded to dates of shorelines in the COAST database. The photography was rectified using ERDAS Imagine 8.5. The procedures used within Imagine resulted in a nearly seamless photo mosaic of the study area for any given date. These procedures were thought to be more accurate than those employed in the creation of the COAST shorelines. This research began to test that idea by comparing the COAST shorelines with the newly created shorelines of the same date. It was found that the differences between these shorelines often exceeded the maximum expected difference. The difference was most pronounced near Oregon Inlet, where the COAST shorelines were generated with a dearth of control points. As a part of this shoreline comparison, the methods used in the mid-1990s rectification of the June 1992 shoreline were compared to this study's rectification of the same shoreline. Differences between the two methods included: choice of basemaps, number of tie points, quality of ground control points, photo correction technique, and shoreline delineation technique. The differences between the two methods could explain up to 85 feet of positional difference between the two shorelines. Finally, fourteen different erosion rates were calculated using linear regression and endpoint methods.

Regression rates found using the new shorelines were substantially different than rates which used COAST shorelines of the same date. It was found that the new rectification technique resulted in shorelines shifted seaward from COAST shorelines for older dates and landward for the more recent dates. This greatly affected the calculated erosion rates. However, when a rate found with all 11 COAST shorelines was compared to one found using all new shorelines and the 1949 T-sheet, the difference was frequently negligible. Endpoint rates over the same span of time were similar to the regression rates, though much more variable.

These results suggested that a governmental agency, like the Division of Coastal Management, likely would not find it worthwhile to rectify large amounts of historical photography in order to calculate erosion rates. The COAST data, when combined with recent shorelines, should suffice for approximate erosion rate calculations. However, consideration should be given to using linear regression over the endpoint method in order to reduce variability in erosion rates. The value of the ERDAS Imagine procedure lies in areas where the COAST shorelines are of questionable quality. Specifically, near inlets and in other areas with few control points, the Imagine technique will result in considerably more accurate shorelines than those found with the COAST method. In locations where short-term rates are calculated, such as near inlets, highly accurate shoreline positions are a necessity. Finally, since photogrammetric work in future shoreline mapping updates will continually become more computer based, an understanding of the procedures used in this study can only aid in the interpretation of future shorelines.

9. REFERENCES

Anders, Fred J. and Mark R Byrnes (1991). Accuracy of Shoreline Change Rates as Determined from Maps and Aerial Photographs. *Shore and Beach*, Vol. 59, No. 1, pp. 17-26.

Anders, Fred J. and Stephen P. Leatherman (1982). Mapping Techniques and Historical Shoreline Analysis – Nauset Spit, Massachusetts. *Geotechnology in Massachusetts*, pp. 501-509.

Benton, Stephen B. (1983). Average Annual Long Term Erosion Rate Update. Methods Report, Division of Coastal Management. North Carolina Department of Natural Resources and Community Development. Raleigh, NC.

Benton, Stephen B., Caroline J. Bellis, Margery F. Overton, John S. Fisher, James L. Hench, and Robert Dolan (1997). North Carolina Long Term Average Annual Rates of Shoreline Change: Methods Report 1992 Update. North Carolina Department of Environment, Health, and Natural Resources, Division of Coastal Management. Raleigh, NC.

Benton, Stephen B. (2002). Personal communication.

Cleary, William J. and Tara P. Marden (1999). Shifting Shorelines: A Pictorial Atlas of North Carolina Inlets. North Carolina Sea Grant. Raleigh, NC.

Crowell, Mark and Michael K. Buckley (1992). Calculating Erosion Rates: Using Long-term Data to Increase Confidence. *Coastal Zone Management*, pp. 117-129.

Dolan, Robert, Bruce Hayden, and Jeffrey Heywood (1978). Analysis of Coastal Erosion and Storm Surge Hazards. *Coastal Engineering*, Vol. 2, pp. 41-53.

Dolan, Robert, Bruce Hayden, and Jeffrey Heywood (1978). A New Photogrammetric Method for Determining Shoreline Erosion. *Coastal Engineering*, Vol. 2, pp. 21-39.

Dolan, Robert, Bruce P. Hayden, Paul May, and Suzette May (1980). The Reliability of Shoreline Change Measurements from Aerial Photographs. *Shore and Beach*, Vol. 48, No. 10, pp. 22-29.

Dolan, Robert, Michael S. Fenster, and Stuart J. Holme (1991). Temporal Analysis of Shoreline Recession and Accretion. *Journal of Coastal Research*, Vol. 7, No. 3, pp.723-744.

Dolan, Robert, Michael S. Fenster, and Stuart J. Holme (1992). Spatial Analysis of Shoreline Recession and Accretion. *Journal of Coastal Research*, Vol. 8, No. 2, pp. 263-285.

ERDAS website (2002). www.support.erdas.com

Everts, C.H. and P.N. Gibson (1983). Shoreline Change Analysis – One Tool for Improving Coastal Zone Decisions. Sixth Australian Conference on Coastal and Ocean Engineering, pp. 122-131.

Falkner, Edgar (1995). Aerial Mapping: Methods and Applications. CRC Press. Boca Raton, FL.

Fenster, Michael S. and Robert Dolan (1994). Large-scale Reversals in Shoreline Trends Along the U.S. mid-Atlantic Coast. *Geology*, Vol. 22, pp. 543-546.

Fenster, Michael S., Robert Dolan, and R.A. Morton (2001). Coastal Storms and Shoreline Change: Signal or Noise? *Journal of Coastal Research*, Vol. 17, No. 3, pp. 714-720.

Foster, Emmett R. and Rebecca J. Savage (1989). Methods of Historical Shoreline Analysis. *Coastal Zone '89*, Vol. 5, pp. 4434-4449.

Galgano, Francis A. and Stephen P. Leatherman (1991). Shoreline Change Analysis: A Case Study. *Coastal Sediments*, Vol. 1, pp. 1043-1053.

Gorman, Laurel, Andrew Morang, and Robert Larson (1998). Monitoring the Coastal Environment; Part IV: Mapping, Shoreline Change, and Bathymetric Analysis. *Journal of Coastal Research*, Vol. 14, No. 1, pp.61-92.

Greve, C. W. (1996). Digital Photogrammetry: An Addendum to the Manual of Photogrammetry. American Society of Photogrammetry and Remote Sensing, Bethesda, MD.

Hiland, Matteson W., Mark R. Byrnes, Randolph A. McBride, and Farrell W. Jones (1993). Change Analysis and Information Management for Coastal Environments. *MicroStation Manager*, Vol. 3, No. 3.

Honeycutt, Maria G., Mark Crowell, and Bruce C. Douglas (2001). Shoreline Position Forecasting: Impact of Storms, Rate-Calculation Methodologies, and Temporal Scales. *Journal of Coastal Research*, Vol. 17, No. 3, pp. 721-730.

Houlahan, John M. (1989). Comparison of State Construction Setbacks to Manage Development in Coastal Hazard Areas. *Coastal Management*, Vol. 17, No. 3, pp. 219-228.

Johnston, Keith (2002). Personal communication.

Langfelder, Leonard J., Donald B. Stafford, and Michael Amein (1970). *Journal of the Waterways and Harbors Division, Proceedings of the American Society of Civil Engineers*, Vol. 96, No. WW2, pp. 531-545.

Leatherman, Stephen P. (1983). Shoreline Mapping: A Comparison of Techniques. *Shore and Beach*, pp. 28-33.

Moore, L. J. (2000). Shoreline Mapping Techniques. *Journal of Coastal Research*, Vol. 16, No. 1, pp. 111-124.

North Carolina Division of Coastal Management (NC DCM) website (2002). http://www.dcm2.enr.state.nc.us

North Carolina State Climate Office website (2002). www.nc-climate.ncsu.edu

Overton, Margery F. and John S. Fisher (1996). Shoreline Analysis Using Digital Photogrammetry. Coastal Engineering 1996, Proceedings of the 25th International Conference, ASCE, Vol. 3, pp. 3750-3761.

Overton, Margery F. and John S. Fisher (2001). Shoreline Monitoring at Oregon Inlet Terminal Groin, Report 21, August-December 2001. North Carolina State University. Raleigh, NC.

Pajak, Mary Jean and Stephen Leatherman (2002). The High Water Line as Shoreline Indicator. *Journal of Coastal Research*, Vol. 18, No. 2, pp. 329-337.

Slama, Chester C., Charles Theurer, and Soren W. Henriksen (1980). Manual of Photogrammetry, 4th Edition. American Society of Photogrammetry, Falls Church, VA.

Smith, George L. and Gary A. Zarillo (1990). Calculating Long-term Shoreline Recession Rates Using Aerial Photographic and Beach Profiling Techniques. *Journal of Coastal Research*, Vol. 6, No. 1, pp. 111-120.

Stafford, Donald B. and Jay Langfelder (1971). Air Photo Survey of Coastal Erosion. *Photogrammetric Engineering*, pp. 565-575.

U.S. Army Corps of Engineers, Field Research Facility website (2002). www.frf.usace.army.mil

The Weather Channel website (2002). www.weather.com

APPENDIX A

Coordinates (NC State Plane feet, NAD83) and Descriptions of Ground Control Points Used in Triangulation.

Table A-1. Coordinates and descriptions of GCPs used in triangulation.

Photo Date	GCP number	X coordinate	Y coordinate	Description	Photo number
March 14, 1962	172	3023576.563	762755.438	corner on dock	128
	171	3023683.627	763351.659	road intersection	128
	173	3022710.965	763538.364	estuarine shoreline feature	128
	174	3022381.127	766970.652	estuarine shoreline feature	130
	175	3022243.114	767131.202	estuarine shoreline feature	130
	176	3022397.266	767017.517	estuarine shoreline feature	130
	177	3021189.023	768383.973	estuarine shoreline feature	131
	178	3021342.884	769098.787	estuarine shoreline feature	131
	179	3021177.832	769530.628	estuarine shoreline feature	131
	183	3021177.813	769530.563	estuarine shoreline feature	132
	181	3020037.377	772846.297	estuarine shoreline feature	132
	185	3020037.438	772846.313	estuarine shoreline feature	133
	13	3019143.313	777226.188	corner on driveway	134
	46	3019387.438	777395.938	corner on sidewalk	134
	48	3018867.938	777710.563	road intersection	134
	58	3018286.813	780288.438	corner of fenceline	135
	138	3017875.063	780525.563	base of light pole	135
December 5, 1962	169	3023450.813	762137.188	corner of bulkhead	79
	30	3023576.620	762755.196	corner of pier	79
	84	3022263.110	767369.949	estuarine shoreline feature	80
	85	3022379.456	766972.278	estuarine shoreline feature	80
	86	3021566.668	766356.714	estuarine shoreline feature	80
	128	3022263.063	767369.938	estuarine shoreline feature	81
	130	3020071.870	774412.091	road intersection	82
	170	3020071.688	774411.938	road intersection	83
	171	3019385.563	777400.813	corner of sidewalk	83
	172	3019142.813	777225.938	corner on driveway	83
	173	3018868.563	777711.188	road intersection	84
	174	3018157.836	778922.548	road intersection	84
	175	3018287.188	780288.313	corner of fenceline	84
	177	3018094.580	780170.588	corner of fenceline	84
	179	3017850.401	780581.662	road intersection	85
	178	3016278.347	780989.419	parking lot	85
November 6, 1972	36	3030381.377	752075.547	parking lot	136
	37	3030778.866	751935.038	road intersection	136
	39	3023450.813	762137.188	corner of bulkhead	138
	40	3023576.563	762755.313	corner of dock	138
	41	3024073.774	764102.892	road intersection	138
	42	3023577.250	762754.750	corner of dock	139
	43	3023450.813	762137.188	corner of bulkhead	139
	44	3024073.750	764102.750	road intersection	139
	45	3030104.406	752019.950	southern end of bridge	136
	52	3020053.108	774474.703	road intersection	140

Table A-1. Coordinates and descriptions of GCPs used in triangulation.

Photo Date	GCP number	X coordinate	Y coordinate	Description	Photo number
	53	3020073.250	774424.250	road intersection	140
	54	3020053.250	774474.750	road intersection	141
	55	3020073.750	774423.750	road intersection	141
	56	3019072.750	777221.250	road intersection	141
	57	3019081.750	777191.250	road intersection	141
	58	3019359.313	777291.938	road in campground	141
	59	3018838.092	777750.352	road intersection	141
	60	3019072.750	777221.250	road intersection	142
	61	3019081.750	777190.750	road intersection	142
	62	3019359.313	777291.938	road in campground	142
	63	3018126.305	778963.039	road intersection	142
	64	3017370.250	779899.750	road intersection	142
	66	3017852.811	780527.807	road intersection	143
	68	3017798.042	780649.342	road intersection	143
	69	3017992.457	780544.238	corner of building	143
	70	3029088.580	754460.332	point on road	137
	71	3029056.580	754671.332	road intersection	137
October 21, 1980	103	3023450.313	762137.438	corner of bulkhead	3874
	103	3023450.313	762137.438	corner of bulkhead	3875
	104	3023674.984	762707.016	corner of pier	3874
	104	3023674.984	762707.016	corner of pier	3875
	105	3031040.849	752528.804	corner of building	3874
	106	3023162.787	762591.918	corner of pier	3875
	107	3018026.332	780362.577	corner of building	3876
	107	3018026.332	780362.577	corner of building	3879
	108	3018366.578	780050.516	corner of house	3876
	108	3018366.578	780050.516	corner of house	3879
	109	3017446.168	777868.837	estuarine shoreline feature	3876
	109	3017446.168	777868.837	estuarine shoreline feature	3879
September 19, 1984	118	3023450.938	762137.688	corner of bulkhead	271
	118	3023450.938	762137.688	corner of bulkhead	272
	118	3023450.938	762137.688	corner of bulkhead	273
	119	3030985.063	752554.688	corner of building	271
	120	3023439.563	762124.313	corner of bulkhead	271
	121	3023639.313	762725.313	corner of pier	272
	121	3023639.313	762725.313	corner of pier	273
	123	3018653.563	778769.438	corner of building	274
	123	3018653.563	778769.438	corner of building	275
	124	3017708.896	780575.771	corner of house	274
	124	3017708.896	780575.771	corner of house	275
	125	3017800.591	781069.985	corner of house	274
	126	3017831.626	781312.625	corner of house	275
	127	3023682.575	762705.410	corner of pier	272

Table A-1. Coordinates and descriptions of GCPs used in triangulation.

Photo Date	GCP number	X coordinate	Y coordinate	Description	Photo number
	127	3023682.575	762705.410	corner of pier	273
October 1, 1986	2	3023451.438	762137.188	corner of bulkhead	64
	4	3023613.450	762690.190	corner of pier	65
	5	3023675.701	762708.611	corner of pier	65
	6	3018653.576	778769.000	corner of house	68
	7	3018606.260	778749.471	corner of house	68
	9	3018606.372	778749.360	corner of house	69
	10	3017708.663	780575.695	corner of house	69
	184	3023214.328	767059.637	vegetation feature	65
	184	3023214.328	767059.637	vegetation feature	66
	185	3019929.940	774497.359	road intersection	67
	185	3019929.940	774497.359	road intersection	68
June 17, 1992	220	3031089.545	752442.512	corner of fenceline	646
	221	3031020.177	752365.109	monument/survey marker	646
	222	3030674.050	752112.902	line in parking lot	646
	223	3031089.545	752442.512	corner of fenceline	647
	225	3030721.010	752075.673	line in parking lot	647
	227	3030103.556	752018.161	southern edge of bridge	647
	224	3031089.688	752442.438	corner of fenceline	648
	226	3030103.438	752018.188	southern edge of bridge	648
	228	3030721.063	752075.688	line in parking lot	648
	229	3023919.063	762029.563	northern end of bridge	649
	230	3023941.438	762029.063	northern end of bridge	649
	231	3023931.188	760798.313	feature on bridge	649
	233	3023919.063	762029.563	northern end of bridge	650
	232	3023941.438	762029.063	northern end of bridge	650
	234	3023450.938	762136.688	corner of bulkhead	650
	236	3023919.188	762029.563	northern end of bridge	651
	235	3023941.438	762028.938	northern end of bridge	651
	237	3023450.938	762136.813	corner of bulkhead	651
	238	3024074.063	764102.688	point in parking lot	652
	239	3023985.188	764124.938	point in parking lot	652
	240	3024185.813	764178.313	point in parking lot	652
	241	3020071.750	774412.250	vegetation feature	653
	242	3019947.563	774517.438	vegetation feature	653
	243	3020152.813	774353.563	vegetation feature	653
	244	3019239.313	776498.563	line on road	654
	245	3019038.938	777165.813	line on driveway	654
	246	3019383.688	777404.188	corner of sidewalk	654
	247	3019039.063	777165.688	line on driveway	655
	248	3019383.813	777404.063	corner of sidewalk	655
	249	3018287.438	780288.188	corner of fenceline	655

APPENDIX B

Images of Final Photo Mosaics
for Seven Photo Dates

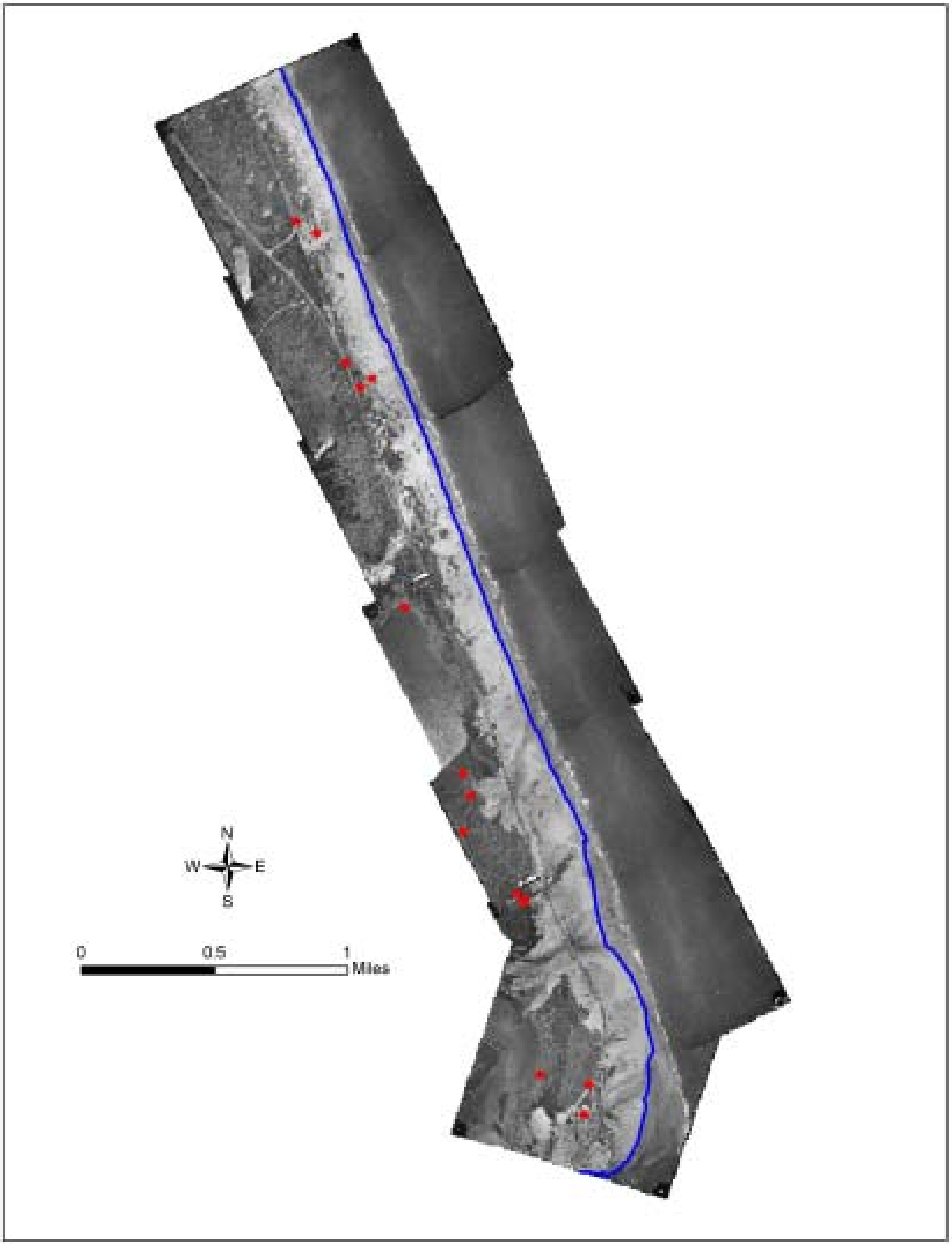

Figure A-1. Final mosaic and GCPs for March 14, 1962.

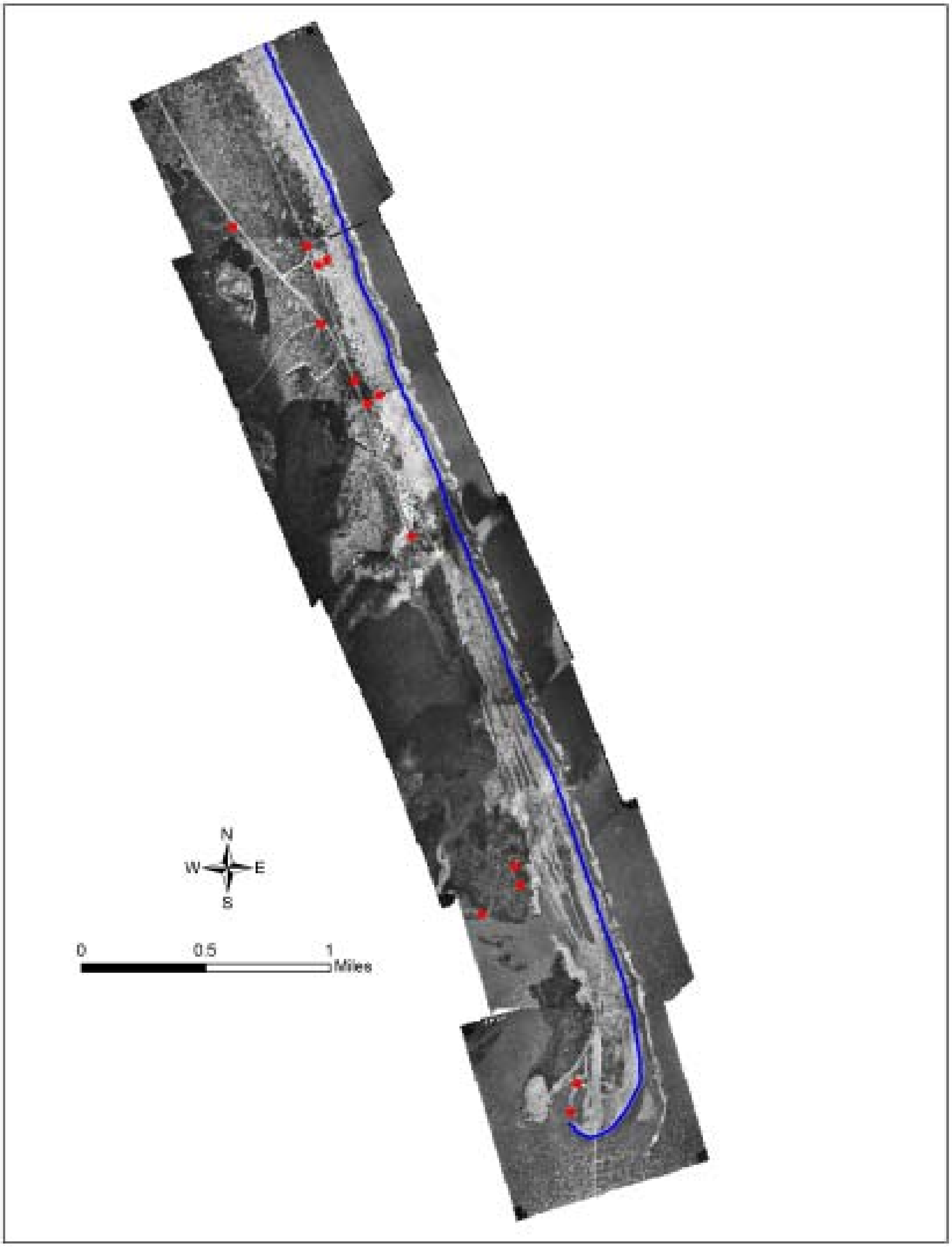

Figure A-2. Final mosaic and GCPs for December 5, 1962.

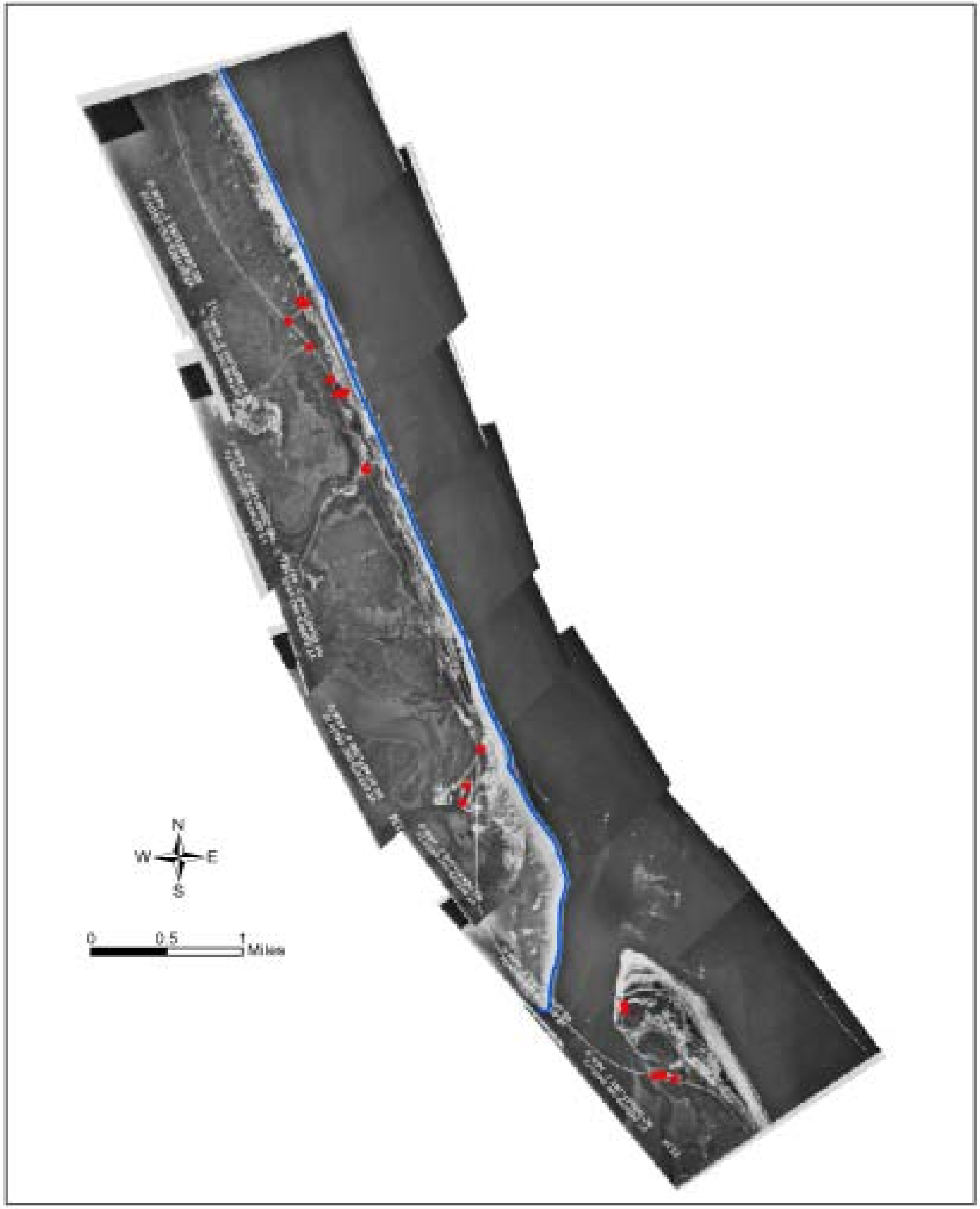

Figure A-3. Final mosaic and GCPs for November 6, 1972.

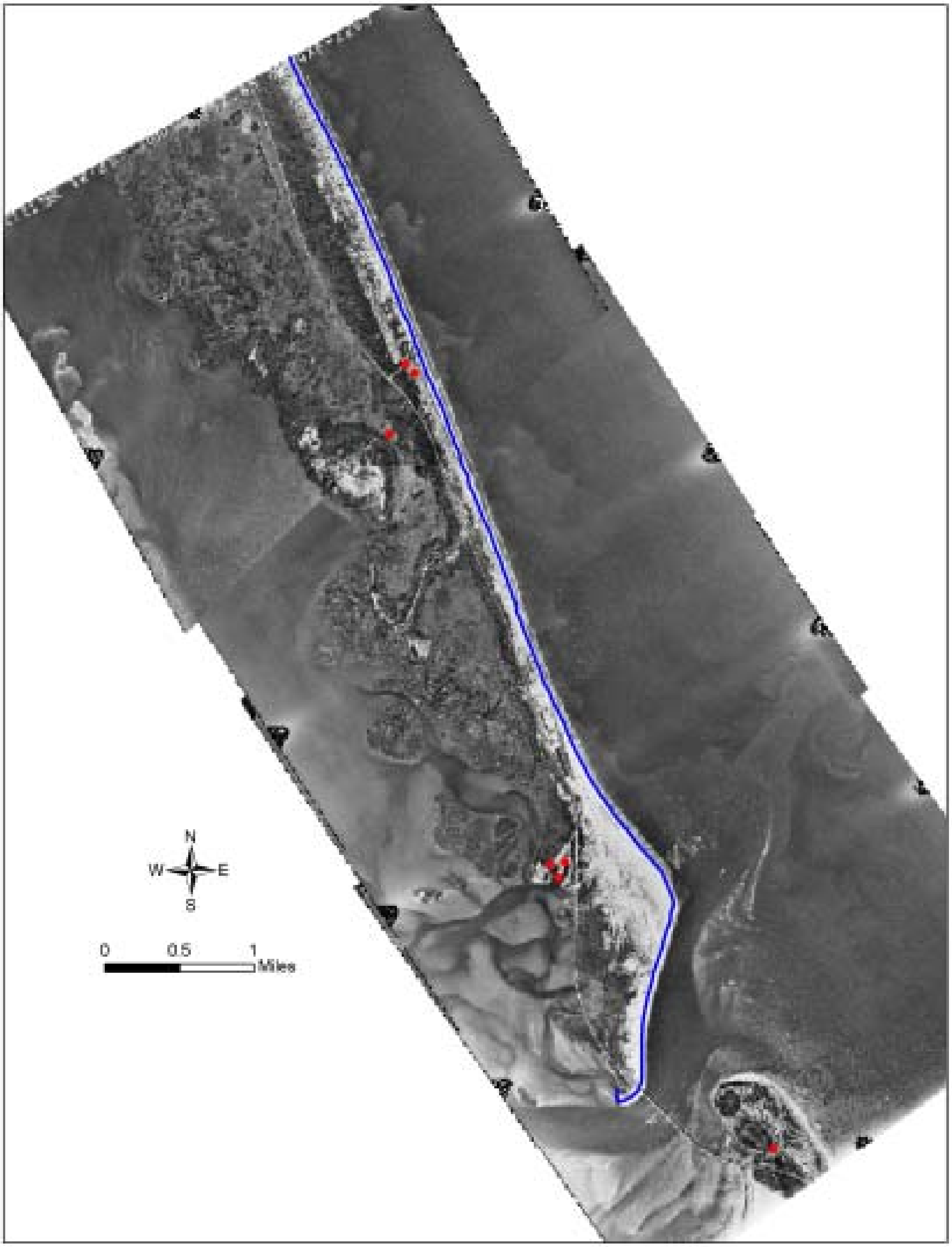

Figure A-4. Final mosaic and GCPs for October 21, 1980.

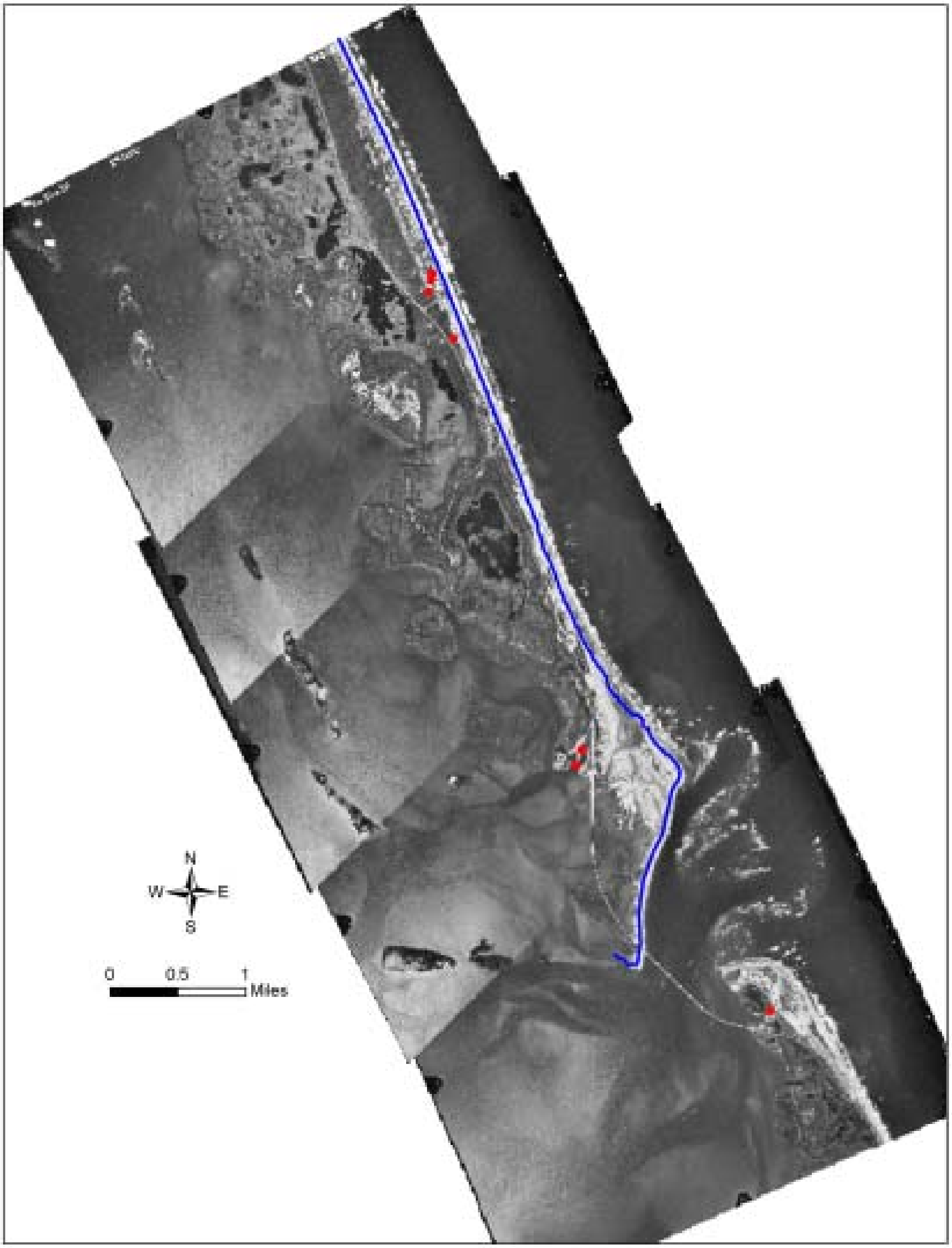

Figure A-5. Final mosaic and GCPs for September 19, 1984.

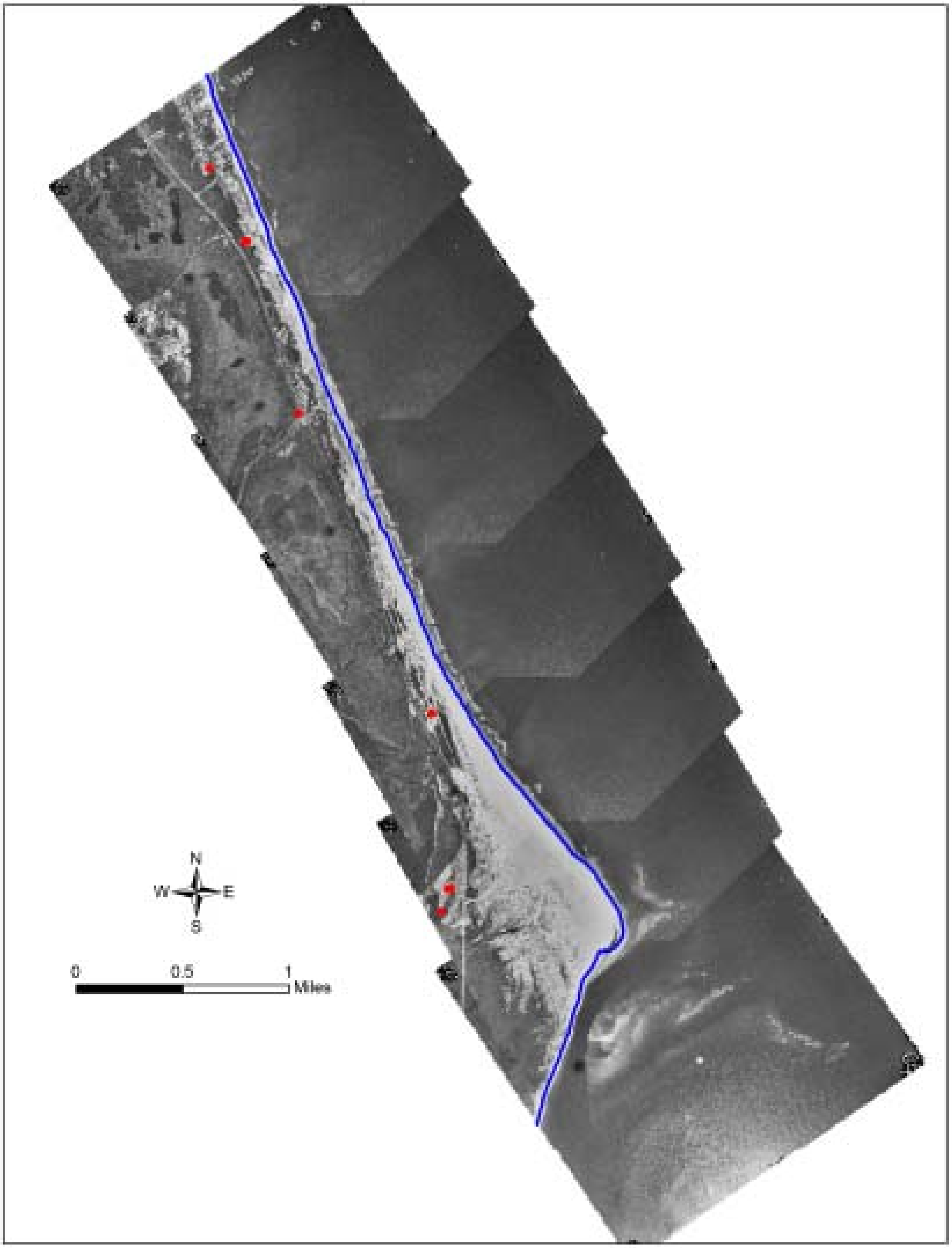

Figure A-6. Final mosaic and GCPs for October 1, 1986.

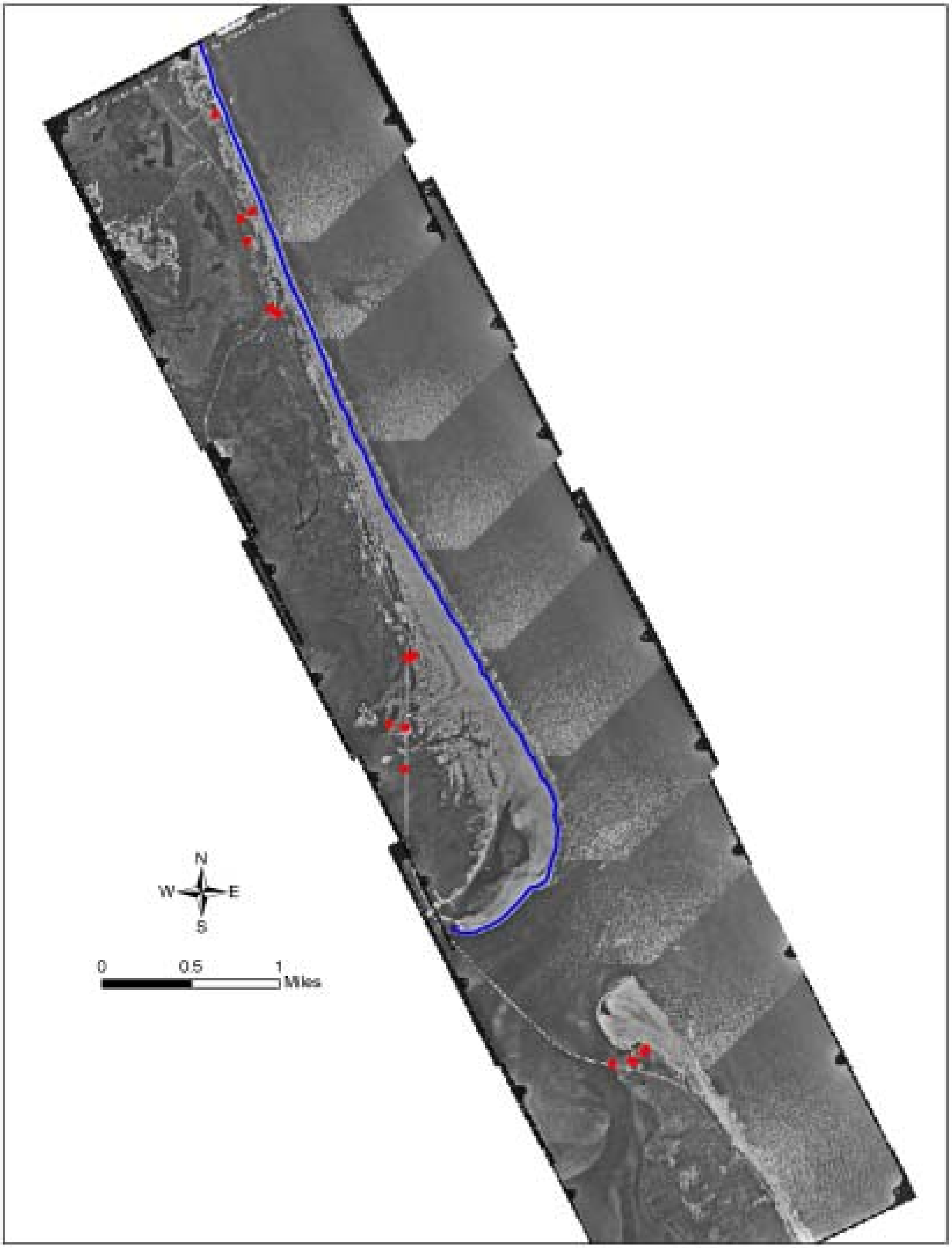

Figure A-7. Final mosaic and GCPs for June 17, 1992.

APPENDIX C

Distances From Baseline for All Study Shorelines

Table A-2. Distances from baseline (feet) for all study shorelines.

Transect	1-Dec-49	1-Jul-45	10-Oct-58	13-Mar-62	13-Dec-62	3-Oct-68	4-Jun-74	21-Oct-80	19-Sep-84	18-Aug-86
number	T-sheet	COAST	COAST	COAST	COAST	COAST	COAST	COAST	COAST	COAST
117	1359	1212	1381	1460	1336	1418	1530	1504	1610	
118	1357	1190	1375	1446	1347	1429	1532	1506	1614	
119	1357	1175	1363	1442	1360	1436	1532	1510	1616	
120	1357	1177	1332	1460	1378	1430	1517	1515	1611	
121	1357	1180	1319	1466	1398	1425	1508	1519	1610	
122	1353	1183	1346	1427	1416	1419	1510	1511	1624	
123	1340	1181	1366	1404	1435	1416	1510	1510	1635	
124	1339	1167	1368	1422	1445	1418	1495	1521	1633	
125	1340	1157	1370	1444	1448	1417	1483	1531	1634	1599
126	1341	1151	1365	1471	1426	1402	1468	1539	1632	1603
127	1339	1153	1359	1496	1415	1392	1462	1546	1634	1607
128	1334	1171	1354	1514	1433	1387	1473	1537	1638	1608
129	1320	1186	1344	1527	1449	1383	1480	1528	1642	1611
130	1306	1188	1322	1512	1451	1385	1474	1516	1643	1623
131	1294	1195	1311	1507	1461	1383	1465	1511	1644	1632
132	1289	1206	1329	1525	1488	1361	1443	1516	1646	1620
133	1283	1214	1345	1544	1511	1343	1431	1520	1648	1610
134	1276	1216	1347	1555	1522	1338	1449	1511	1656	1608
135	1270	1217	1349	1562	1533	1337	1464	1506	1665	1608
136	1264	1212	1343	1557	1544	1348	1458	1514	1680	1603
137	1259	1207	1338	1555	1551	1365	1454	1517	1693	1605
138	1255	1201	1332	1566	1546	1399	1456	1505	1688	1624
139	1256	1198	1337	1576	1537	1426	1443	1491	1626	1623
140	1257	1200	1344	1626	1535	1420	1466	1492	1626	1621
141	1265	1188	1352	1675	1538	1410	1491	1492	1628	1620
142	1269	1204	1365	1687	1538	1410	1516	1494	1631	1623
143	1271	1229	1382	1654	1538	1418	1540	1499	1636	1631
144	1274	1246	1391	1614	1556	1434	1558	1504	1648	1634
145	1277	1254	1391	1565	1598	1459	1566	1507	1664	1629
146	1281	1260	1399	1549	1613	1466	1575	1518	1672	1630
147	1285	1260	1415	1574	1597	1450	1583	1538	1669	1639
148	1281	1260	1427	1589	1584	1448	1599	1554	1669	1635
149	1316	1261	1436	1589	1576	1465	1624	1565	1674	1616
150	1303	1268	1444	1589	1580	1470	1634	1576	1684	1610
151	1331	1285	1453	1589	1597	1461	1626	1584	1698	1621
152	1337	1290	1454	1582	1601	1458	1622	1595	1709	1635
153	1339	1281	1446	1566	1593	1458	1622	1610	1713	1648
154	1339	1278	1442	1567	1585	1462	1615	1610	1722	1663
155	1332	1278	1442	1592	1577	1470	1599	1592	1739	1681
156	1323	1274	1443	1599	1569	1478	1593	1587	1748	1695
157	1313	1266	1443	1583	1561	1487	1602	1594	1750	1703
158	1303	1263	1446	1577	1561	1492	1603	1599	1761	1715
159	1297	1263	1454	1586	1569	1493	1595	1602	1780	1728
160	1296		1460	1579	1578	1500	1599	1610	1784	1737
161	1295		1460	1555	1586	1517	1615	1625	1769	1742
162	1294		1468	1545	1599	1533	1627	1636	1764	1749
163	1294		1484	1554	1616	1550	1636	1641	1767	1756
164	1292		1501	1555	1628	1555	1641	1649	1768	1762
165	1290		1518	1547	1636	1547	1642	1661	1766	1769
166	1288		1522	1546	1642	1554	1660	1662	1766	1773
167	1287		1514	1555	1642	1578	1701	1649	1768	1773
168	1288	1228	1504	1570	1645	1586	1709	1645	1775	1772
169	1285	1219	1487	1595	1653	1569	1677	1652	1785	1770
170	1282	1212	1479	1598	1655	1564	1677	1660	1789	1766
171	1279	1203	1479	1573	1646	1572	1718	1670	1786	1758
172	1277	1200	1479	1561	1658	1577	1734	1674	1783	1750
173	1276	1200	1479	1561	1691	1578	1718	1671	1780	1742
174	1271	1203	1479	1561	1712	1593	1709	1662	1781	1736
175	1142	1081	1354	1436	1592	1489	1583	1526	1660	1606
176	1141	1097	1360	1449	1601	1522	1588	1523	1675	1611
177	1143	1093	1366	1522	1575	1512	1585	1572	1701	1627
178	1149	1092	1373	1586	1555	1507	1586	1620	1724	1642
179	1156	1082	1396	1599	1577	1546	1599	1639	1734	1655

Table A-2. Distances from baseline (feet) for all study shorelines.

Transect	1-Dec-49	1-Jul-45	10-Oct-58	13-Mar-62	13-Dec-62	3-Oct-68	4-Jun-74	21-Oct-80	19-Sep-84	18-Aug-86
number	T-sheet	COAST	COAST	COAST	COAST	COAST	COAST	COAST	COAST	COAST
180	1158	1072	1418	1614	1598	1580	1616	1655	1746	1670
181	1161	1078	1430	1620	1612	1576	1639	1651	1759	1676
182	1192	1084	1447	1624	1628	1575	1661	1653	1772	1687
183	1210	1080	1470	1613	1651	1572	1684	1682	1788	1703
184	1220	1080	1490	1605	1672	1573	1702	1708	1802	1723
185	1230	1093	1496	1611	1685	1579	1699	1717	1809	1746
186	1240	1108	1501	1615	1700	1585	1702	1731	1817	1763
187	1248	1115	1498	1605	1706	1591	1725	1771	1817	1736
188	1253	1121	1496	1600	1713	1596	1745	1808	1828	1711
189	1251	1127	1486	1630	1726	1592	1751	1817	1878	1691
190	1249	1133	1476	1661	1740	1593	1757	1823	1922	1675
191	1237	1139	1466	1683	1746	1599	1763	1813	1931	1681
192	1238	1145	1456	1711	1753	1606	1769	1811	1940	1689
193	1251	1151	1453	1767	1759	1619	1775	1831	1946	1712
194	1265	1157	1454	1820	1765	1632	1782	1851	1959	1731
195	1278	1153	1477	1859	1775	1629	1795	1860	1982	1730
196	1292	1153	1496	1876	1779	1631	1810	1870	2003	1732
197	1306	1149	1486	1802	1740	1654	1816	1883	2010	1748
198	1315	1149	1478	1738	1703	1674	1822	1897	2021	1762
199	1324	1155	1491	1735	1683	1680	1828	1904	2038	1761
200	1344	1161	1506	1735	1673	1685	1838	1916	2055	1763
201	1353	1167	1512	1742	1703	1681	1868	1939	2069	1779
202	1350	1173	1518	1748	1735	1686	1894	1956	2083	1795
203	1347	1169	1531	1754	1764	1726	1890	1953	2093	1812
204	1350	1169	1547	1756	1795	1758	1891	1950	2104	1826
205	1354	1198	1560	1736	1818	1755	1897	1937	2107	1820
206	1361	1230	1576	1735	1840	1760	1903	1931	2113	1818
207	1374	1226	1589	1824	1863	1800	1909	1943	2116	1824

Table A-2. Distances from baseline (feet) for all study shorelines.

Transect	1-Oct-86	17-Jun-92	14-Mar-62	5-Dec-62	6-Nov-72	21-Oct-80	19-Sep-84	1-Oct-86	17-Jun-92	22-Jul-98
number	COAST	COAST	new	new	new	new	new	new	new	
117	1625	1596	1360	1365	1469	1580	1700	1638	1610	1646
118	1631	1592	1380	1363	1484	1586	1701	1647	1613	1653
119	1642	1596	1381	1372	1480	1579	1711	1662	1607	1651
120	1628	1595	1377	1362	1477	1556	1716	1641	1618	1644
121	1636	1600	1381	1361	1494	1541	1693	1650	1612	1646
122	1632	1616	1382	1362	1484	1558	1713	1635	1632	1652
123	1627	1637	1377	1394	1494	1562	1719	1635	1650	1636
124	1630	1661	1366	1389	1478	1571	1709	1666	1676	1645
125	1618	1677	1376	1381	1471	1595	1710	1651	1702	1646
126	1609	1678	1384	1374	1448	1599	1704	1638	1717	1633
127	1611	1663	1394	1403	1442	1588	1710	1644	1695	1633
128	1614	1650	1405	1425	1426	1606	1729	1654	1689	1635
129	1615	1656	1420	1409	1465	1600	1719	1649	1683	1639
130	1624	1663	1426	1424	1511	1594	1721	1651	1679	1643
131	1613	1682	1463	1453	1540	1605	1737	1649	1680	1656
132	1610	1697	1471	1471	1539	1619	1723	1639	1718	1672
133	1615	1696	1472	1503	1561	1625	1734	1646	1716	1696
134	1620	1697	1492	1515	1559	1601	1726	1648	1714	1702
135	1631	1694	1453	1522	1554	1584	1740	1660	1722	1703
136	1635	1701	1491	1510	1554	1605	1751	1674	1711	1699
137	1614	1706	1492	1495	1563	1601	1758	1651	1716	1697
138	1614	1705	1484	1487	1567	1587	1766	1654	1718	1705
139	1575	1708	1502	1454	1571	1574	1779	1673	1721	1696
140	1595	1705	1513	1474	1593	1574	1762	1694	1716	1697
141	1622	1699	1555	1484	1620	1573	1775	1725	1713	1694
142	1638	1694	1533	1483	1620	1573	1777	1733	1713	1698
143	1637	1692	1551	1489	1627	1590	1777	1716	1712	1702
144	1627	1693	1540	1520	1629	1600	1773	1699	1711	1706
145	1630	1699	1508	1544	1654	1629	1773	1707	1710	1704
146	1631	1705	1499	1560	1658	1630	1776	1708	1707	1710
147	1614	1705	1499	1567	1656	1610	1789	1689	1705	1713
148	1594	1707	1516	1562	1643	1633	1792	1662	1712	1720
149	1588	1710	1502	1559	1659	1640	1794	1665	1715	1719
150	1588	1720	1498	1571	1660	1619	1818	1651	1722	1718
151	1584	1730	1505	1545	1661	1626	1798	1656	1740	1730
152	1588	1737	1513	1558	1666	1672	1802	1654	1744	1732
153	1593	1738	1525	1578	1659	1698	1796	1664	1741	1740
154	1599	1731	1514	1560	1644	1700	1790	1676	1730	1749
155	1621	1734	1530	1525	1638	1683	1829	1706	1733	1766
156	1656	1749	1534	1524	1642	1662	1835	1730	1757	1757
157	1686	1759	1533	1541	1665	1683	1836	1755	1764	1756
158	1695	1767	1523	1540	1674	1717	1825	1766	1782	1756
159	1680	1778	1543	1543	1653	1726	1851	1745	1789	1772
160	1688	1785	1528	1539	1643	1707	1845	1758	1792	1775
161	1715	1788	1538	1527	1654	1701	1838	1773	1817	1770
162	1728	1792	1540	1558	1673	1703	1840	1782	1797	1782
163	1730	1797	1557	1560	1676	1696	1835	1792	1812	1799
164	1734	1791	1575	1577	1684	1703	1844	1790	1809	1776
165	1738	1778	1561	1612	1700	1715	1843	1796	1812	1781
166	1732	1772	1568	1613	1695	1719	1842	1781	1794	1793
167	1741	1767	1600	1615	1686	1710	1845	1792	1779	1777
168	1748	1759	1606	1624	1704	1690	1848	1804	1771	1781
169	1730	1751	1604	1607	1709	1686	1849	1782	1761	1784
170	1727	1746	1597	1598	1721	1695	1846	1771	1759	1767
171	1727	1745	1612	1577	1726	1714	1841	1775	1754	1785
172	1711	1745	1627	1586	1729	1723	1851	1766	1741	1773
173	1717	1741	1626	1605	1739	1723	1847	1755	1748	1760
174	1728	1734	1628	1623	1719	1720	1854	1786	1745	1770
175	1595	1606	1509	1504	1607	1590	1727	1646	1622	1641
176	1611	1608	1529	1497	1643	1596	1747	1660	1630	1631
177	1609	1608	1524	1508	1654	1616	1772	1662	1632	1639
178	1640	1614	1531	1514	1644	1642	1783	1686	1636	1639
179	1661	1632	1559	1530	1648	1652	1806	1705	1641	1647

Table A-2. Distances from baseline (feet) for all study shorelines.

Transect number	1-Oct-86 COAST	17-Jun-92 COAST	14-Mar-62 new	5-Dec-62 new	6-Nov-72 new	21-Oct-80 new	19-Sep-84 new	1-Oct-86 new	17-Jun-92 new	22-Jul-98
180	1675	1643	1564	1530	1653	1653	1817	1705	1662	1638
181	1698	1649	1579	1545	1669	1677	1823	1732	1680	1647
182	1732	1653	1593	1566	1695	1688	1849	1775	1692	1616
183	1721	1661	1605	1575	1700	1695	1843	1765	1696	1640
184	1709	1665	1616	1585	1699	1716	1858	1763	1714	1646
185	1707	1672	1605	1592	1700	1733	1865	1751	1727	1626
186	1721	1666	1611	1607	1706	1741	1878	1762	1737	1628
187	1746	1664	1617	1652	1706	1778	1869	1796	1742	1652
188	1702	1652	1631	1670	1726	1837	1869	1757	1731	1641
189	1694	1632	1642	1661	1728	1832	1962	1744	1707	1659
190	1715	1636	1656	1667	1746	1830	1976	1756	1705	1682
191	1729	1649	1673	1687	1749	1856	1974	1771	1734	1667
192	1746	1661	1677	1703	1733	1860	2004	1786	1750	1672
193	1753	1669	1688	1718	1745	1869	2044	1795	1765	1674
194	1745	1667	1710	1722	1741	1878	2054	1795	1753	1673
195	1737	1652	1709	1701	1759	1875	2053	1780	1752	1670
196	1747	1629	1696	1733	1776	1878	2039	1801	1715	1671
197	1717	1614	1685	1742	1798	1890	2045	1785	1706	1659
198	1723	1611	1695	1732	1798	1899	2030	1778	1720	1675
199	1750	1613	1698	1737	1793	1912	2046	1780	1723	1676
200	1760	1611	1734	1729	1792	1915	2055	1799	1709	1670
201	1780	1620	1736	1726	1800	1924	2070	1816	1724	1652
202	1810	1622	1719	1740	1781	1941	2088	1825	1715	1632
203	1798	1626	1711	1744	1806	1971	2108	1861	1741	1625
204	1794	1638	1704	1750	1806	1973	2133	1857	1751	1620
205	1812	1640	1720	1775	1801	1962	2122	1855	1748	1615
206	1834	1638	1691	1775	1820	1947	2126	1861	1751	1589
207	1833	1629	1684	1784	1818	1948	2151	1877	1748	1574

APPENDIX D

Calculated Erosion Rates for Study Transects

Table A-3. Calculated erosion rates (ft/yr) for study transects.

Transect	Rate 1	Rate 2	Rate 3	Rate 4	Rate 5	Rate 6	Rate 7	Rate 8	Rate 9	Rate 10	Rate 11	Rate 12	Rate 13	Rate 14
number	positive values signify erosion; negative signify accretion													
117	8.2	5.9	8.8	12.9	7.7	10.5	7.2	8.9	8.2	7.8	8.5	6.1	8.1	7.8
118	8.7	6.1	9.0	12.7	7.8	10.3	7.4	8.8	8.6	7.8	9.0	6.3	8.4	7.9
119	9.0	6.0	9.2	12.8	7.9	10.2	7.4	8.6	8.8	7.8	9.3	6.3	8.7	7.8
120	8.8	5.9	8.0	12.6	7.0	10.4	6.6	8.8	8.4	7.8	9.1	6.2	8.5	7.8
121	8.8	5.9	7.6	12.2	6.7	10.1	6.3	8.7	8.3	7.7	9.1	6.2	8.6	7.7
122	8.8	6.2	8.2	12.4	7.4	10.5	6.9	8.9	8.6	8.0	9.3	6.5	8.7	8.0
123	8.6	6.1	8.4	11.9	7.9	10.3	6.9	8.4	8.7	7.9	9.2	6.7	8.6	7.9
124	9.0	6.3	7.9	12.8	7.8	11.4	6.9	9.2	9.0	8.5	9.8	7.1	8.9	8.5
125	9.2	6.3	7.2	12.7	7.5	11.7	6.6	9.3	9.0	8.6	10.1	7.2	9.0	8.7
126	9.1	6.0	6.9	12.3	7.3	11.8	6.2	9.2	8.9	8.5	10.0	7.1	9.0	8.6
127	9.0	6.0	6.7	11.6	6.9	10.7	5.9	8.4	8.7	8.1	9.9	7.0	8.9	8.3
128	8.7	6.2	5.9	11.5	6.0	10.3	5.2	7.9	8.2	8.1	9.5	7.2	8.5	8.3
129	8.5	6.6	5.3	11.2	5.5	10.0	4.9	7.9	7.9	8.2	9.3	7.5	8.4	8.3
130	8.6	6.9	5.7	10.7	6.0	9.6	5.3	7.6	8.1	8.2	9.3	7.8	8.7	8.3
131	8.7	7.4	5.3	9.6	6.1	8.5	5.6	6.8	8.1	8.1	9.4	8.2	8.9	8.1
132	8.8	7.9	4.3	8.7	5.5	8.5	5.2	6.9	8.0	8.4	9.5	8.7	8.7	8.4
133	9.1	8.5	3.5	8.4	4.7	8.0	4.9	6.8	7.9	8.6	9.5	9.2	8.6	8.5
134	9.2	8.8	3.2	7.3	4.4	7.2	4.7	6.3	7.8	8.4	9.6	9.4	8.5	8.4
135	9.1	8.9	3.1	8.4	4.2	8.2	4.5	7.0	7.7	8.9	9.6	9.6	8.5	8.9
136	9.2	8.9	3.4	8.4	4.4	7.8	4.5	6.5	7.8	8.8	9.7	9.7	8.6	8.8
137	9.3	9.0	3.1	8.3	4.3	7.9	4.3	6.7	7.9	8.9	9.8	9.7	8.6	8.8
138	9.5	9.3	2.8	8.7	4.1	8.3	4.3	7.1	7.9	9.2	10.0	10.0	8.7	9.1
139	9.4	9.0	0.8	9.5	3.1	8.9	3.8	7.4	7.5	9.3	9.8	9.9	8.1	9.2
140	9.4	9.0	0.1	9.0	2.4	8.3	3.1	6.9	7.2	9.1	9.8	9.9	7.9	9.0
141	9.5	8.8	-0.5	8.6	1.5	7.6	2.3	6.2	7.1	8.7	10.1	9.8	7.8	8.6
142	9.3	8.8	-0.4	9.3	1.4	8.2	2.2	6.7	6.9	8.9	9.8	9.8	7.6	8.8
143	8.9	8.9	0.5	8.6	2.1	7.6	2.8	6.2	6.8	8.7	9.4	9.7	7.5	8.6
144	8.7	8.9	1.0	7.8	2.5	7.0	3.2	5.9	6.8	8.5	9.0	9.6	7.3	8.4
145	8.5	8.8	1.6	8.5	3.0	7.3	3.5	6.0	6.8	8.6	8.9	9.6	7.3	8.4
146	8.5	8.8	1.9	8.4	3.2	7.2	3.7	6.0	6.9	8.5	8.9	9.5	7.3	8.3
147	8.5	8.8	1.5	7.9	2.9	6.9	3.5	5.9	6.8	8.4	8.8	9.4	7.2	8.2
148	8.7	9.0	1.2	7.4	2.7	6.6	3.4	5.7	6.8	8.4	8.8	9.5	7.2	8.2
149	8.6	8.3	1.4	7.9	2.9	7.0	3.6	6.0	6.9	8.1	8.8	8.8	7.0	7.9
150	8.5	8.5	1.6	7.7	3.1	7.0	3.6	5.9	6.9	8.2	8.7	9.0	7.0	8.1
151	8.4	8.2	1.4	7.9	3.1	7.6	3.6	6.5	6.8	8.2	8.6	8.7	6.9	8.0
152	8.3	8.1	1.9	7.9	3.4	7.4	3.8	6.3	6.9	8.1	8.6	8.6	7.1	8.0
153	8.6	8.3	2.7	7.5	4.0	6.9	4.4	5.9	7.3	8.0	8.8	8.7	7.5	7.9
154	8.9	8.4	3.1	8.3	4.2	7.3	4.6	6.4	7.5	8.2	9.0	8.7	7.8	8.1
155	9.2	8.9	3.3	9.8	4.2	8.3	4.8	7.2	7.7	8.9	9.2	9.2	8.0	8.8
156	9.1	8.9	4.0	10.1	4.9	8.9	5.0	7.4	7.9	9.2	9.4	9.6	8.3	9.1
157	9.2	9.1	5.3	10.4	5.9	9.0	5.6	7.3	8.4	9.4	9.8	9.9	8.7	9.3
158	9.3	9.3	5.8	11.1	6.3	9.7	5.9	7.7	8.6	9.8	9.9	10.3	8.9	9.7
159	9.6	9.7	5.5	10.6	6.2	9.3	5.9	7.6	8.8	10.0	10.1	10.6	9.1	9.9
160		9.9	5.7	11.0	6.4	9.8	6.0	8.0		10.2	10.0	10.7		10.1
161		9.8	6.6	11.2	7.0	10.3	6.4	8.3		10.4	8.6	10.9		10.3
162		10.0	6.8	10.7	7.1	9.5	6.6	7.8		10.2	8.5	11.0		10.1
163		10.4	6.3	10.3	6.8	9.4	6.5	7.9		10.4	9.2	11.3		10.3
164		10.0	6.2	9.7	6.6	8.8	5.9	7.0		9.9	7.4	11.1		9.8
165		10.1	6.4	9.5	6.4	8.5	5.9	6.8		9.9	6.8	11.2		9.8
166		10.4	6.2	9.0	6.1	7.9	5.9	6.6		9.8	7.3	11.2		9.7
167		10.1	6.1	8.4	5.9	7.1	5.5	5.7		9.3	6.9	10.9		9.2
168	10.4	10.1	5.8	8.2	5.5	6.7	5.2	5.6	9.2	9.2	11.0	11.0	9.1	9.1
169	10.6	10.3	5.0	8.1	4.7	6.7	4.6	5.7	9.0	9.2	11.1	10.9	9.2	9.1
170	10.5	10.0	4.9	8.3	4.5	6.9	4.2	5.6	8.9	9.2	11.0	10.7	9.1	9.0
171	11.0	10.4	5.7	8.6	5.2	6.9	5.0	5.9	9.4	9.4	11.4	11.0	9.4	9.2
172	10.8	10.2	5.4	8.1	5.0	6.3	4.8	5.2	9.3	9.1	11.3	10.7	9.3	8.9
173	10.6	10.0	4.8	7.4	4.3	5.9	4.0	4.7	8.9	8.8	11.1	10.6	9.0	8.6

Table A-3. Calculated erosion rates (ft/yr) for study transects.

Transect	Rate 1	Rate 2	Rate 3	Rate 4	Rate 5	Rate 6	Rate 7	Rate 8	Rate 9	Rate 10	Rate 11	Rate 12	Rate 13	Rate 14
number	positive values signify erosion; negative signify accretion													
174	10.7	10.2	4.4	7.7	3.9	5.8	3.8	4.7	8.8	9.0	11.2	10.9	8.8	8.8
175	10.6	10.3	4.2	7.1	3.7	5.5	3.7	4.4	8.7	8.8	11.0	11.0	8.6	8.6
176	10.1	10.1	4.2	7.4	3.6	5.7	3.3	4.3	8.4	8.8	10.7	10.9	8.3	8.6
177	10.3	10.2	3.9	7.9	3.0	5.8	2.7	4.4	8.4	9.0	10.8	11.0	8.4	8.7
178	10.3	10.1	4.3	8.5	2.8	6.1	2.2	4.3	8.4	9.0	11.0	11.0	8.6	8.8
179	10.7	10.1	4.2	8.3	2.8	5.7	2.1	4.0	8.7	9.0	11.5	11.0	8.7	8.8
180	10.7	9.9	4.1	8.4	2.6	6.1	1.6	4.0	8.8	9.0	11.7	11.0	8.6	8.8
181	10.7	10.0	4.2	8.6	2.7	6.2	1.6	4.0	8.8	9.2	11.8	11.3	8.7	8.9
182	10.0	8.7	4.7	9.2	2.8	6.4	1.0	3.3	8.5	8.6	11.5	10.5	8.4	8.3
183	10.5	8.8	4.7	8.4	2.8	5.9	1.3	3.3	8.9	8.4	11.8	10.3	8.6	8.2
184	10.7	8.8	4.7	8.4	2.7	6.0	1.2	3.3	8.9	8.4	11.9	10.3	8.7	8.2
185	10.1	8.1	4.4	8.5	2.5	6.3	0.7	3.1	8.5	8.2	11.5	9.9	8.4	8.0
186	9.8	8.0	4.6	8.5	2.3	6.3	0.4	3.0	8.3	8.1	11.2	9.8	8.3	7.9
187	10.1	8.3	5.5	8.3	2.8	5.8	0.9	2.7	8.6	8.1	11.4	10.0	8.5	8.0
188	9.8	8.0	5.1	7.4	2.3	4.8	0.5	1.8	8.3	7.5	10.9	9.6	8.1	7.4
189	10.0	8.4	4.9	8.5	1.4	4.9	-0.1	2.0	8.1	7.8	10.8	9.6	8.0	7.6
190	10.4	8.9	5.0	8.5	1.2	4.7	-0.2	2.1	8.2	8.0	11.0	9.9	8.2	7.8
191	10.0	8.8	4.7	8.2	1.0	4.7	-0.6	1.6	8.0	8.1	10.9	10.3	8.0	7.9
192	9.9	8.9	4.4	8.5	0.8	5.0	-0.9	1.7	7.9	8.3	10.9	10.5	8.1	8.2
193	9.9	8.7	3.4	8.8	-0.1	5.2	-1.7	1.6	7.6	8.2	10.9	10.3	8.0	8.1
194	9.7	8.4	2.2	8.5	-1.2	4.6	-2.8	1.1	7.2	7.8	10.7	9.9	7.7	7.7
195	9.7	8.1	1.4	8.6	-2.3	4.8	-3.7	1.3	6.8	7.7	10.6	9.5	7.3	7.6
196	9.8	7.8	1.6	8.5	-2.8	4.0	-4.1	0.7	6.7	7.2	10.6	9.1	7.1	7.0
197	9.6	7.3	3.8	8.4	-1.1	3.8	-2.8	0.4	7.2	6.8	10.3	8.5	7.5	6.6
198	9.9	7.4	6.5	8.1	1.0	3.9	-0.9	0.7	8.0	6.8	10.5	8.5	8.2	6.6
199	9.8	7.3	7.8	8.3	1.9	3.9	-0.3	0.7	8.3	6.8	10.5	8.4	8.4	6.6
200	9.6	6.7	8.7	8.2	2.3	3.4	-0.2	0.1	8.3	6.2	10.3	7.8	8.3	6.1
201	9.1	6.1	8.7	8.9	2.2	4.0	-0.8	0.1	8.1	6.2	10.1	7.5	8.2	6.1
202	8.7	5.8	8.8	9.6	2.0	4.2	-1.5	-0.1	7.8	6.1	9.9	7.3	8.0	6.0
203	8.6	5.7	7.9	11.0	1.3	5.4	-2.1	0.3	7.6	6.6	9.9	7.6	7.8	6.5
204	8.5	5.6	7.3	11.4	0.9	5.7	-2.6	0.4	7.4	6.7	9.9	7.6	7.6	6.6
205	7.8	5.4	7.5	10.2	1.1	4.8	-2.6	-0.4	7.0	6.2	9.3	7.4	7.2	6.1
206	6.8	4.7	7.5	10.9	0.9	5.4	-3.2	-0.2	6.3	6.1	8.5	7.0	6.5	5.9
207	6.6	4.1	5.1	11.6	-1.4	5.7	-5.3	-0.3	5.5	5.9	8.3	6.6	5.7	5.7